Syst. Biol. 66(5):715–736, 2017

DOI:10.1093/sysbio/syw114
Advance Access publication December 21, 2016

How Do Cold-Adapted Plants Respond to Climatic Cycles? Interglacial Expansion Explains Current Distribution and Genomic Diversity in *Primula farinosa* L.

SPYROS THEODORIDIS[1,2,*], CHRISTOPHE RANDIN[3,4], PETER SZÖVÉNYI[1], FLORIAN C. BOUCHER[1,5], THEOFANIA S. PATSIOU[1,2,3], AND ELENA CONTI[1,2]

[1]*Department of Systematic and Evolutionary Botany, University of Zurich, CH-8008 Zurich, Switzerland;* [2]*Zurich-Basel Plant Science Center, CH-8092 Zurich, Switzerland;* [3]*Institute of Botany, University of Basel, CH-4056 Basel, Switzerland;* [4]*Department of Ecology & Evolution, University of Lausanne, CH-1015 Lausanne, Switzerland; and* [5]*Department of Botany and Zoology, University of Stellenbosch, 7602 Matieland, South Africa*
[*]*Correspondence to be sent to: Department of Systematic and Evolutionary Botany, University of Zurich, Zollikerstrasse 107, CH-8008 Zurich, Switzerland; E-mail: spyros.theodoridis@systbot.uzh.ch.*

Received 8 March 2016; reviews returned 22 June 2016; accepted 14 December 2016
Associate Editor: Roberta Mason Gamer

Abstract.—Understanding the effects of past climatic fluctuations on the distribution and population-size dynamics of cold-adapted species is essential for predicting their responses to ongoing global climate change. In spite of the heterogeneity of cold-adapted species, two main contrasting hypotheses have been proposed to explain their responses to Late Quaternary glacial cycles, namely, the interglacial contraction versus the interglacial expansion hypotheses. Here, we use the cold-adapted plant *Primula farinosa* to test two demographic models under each of the two alternative hypotheses and a fifth, null model. We first approximate the time and extent of demographic contractions and expansions during the Late Quaternary by projecting species distribution models across the last 72 ka. We also generate genome-wide sequence data using a Reduced Representation Library approach to reconstruct the spatial structure, genetic diversity, and phylogenetic relationships of lineages within *P. farinosa*. Finally, by integrating the results of climatic and genomic analyses in an Approximate Bayesian Computation framework, we propose the most likely model for the extent and direction of population-size changes in *P. farinosa* through the Late Quaternary. Our results support the interglacial expansion of *P. farinosa*, differing from the prevailing paradigm that the observed distribution of cold-adapted species currently fragmented in high altitude and latitude regions reflects the consequences of postglacial contraction processes. [Approximate Bayesian computation; climate change; hindcasting; Late Quaternary glacial cycles; paleoclimate; Reduced Representation Library; species distribution models.]

The responses of species and communities to Quaternary climatic oscillations have represented one of the main research topics in biogeography for over a century (Darwin 1859; Willis and Whittaker 2000; Hewitt 2000, 2004; Taberlet and Cheddadi 2003), recently acquiring heightened relevance in relation to current trends of global warming (Etterson 2008; Lavergne et al. 2010). Species may react to climate change by expanding or contracting their distributional ranges. Range dynamics may in turn drive processes of hybridization, speciation, and extinction that vary both temporally and spatially among species adapted to different climates (Hewitt 1996; Stewart et al. 2010; Dawson et al. 2011). In the European subcontinent, the prevailing paradigm for species responses to Quaternary glacial cycles has largely relied on studies of temperate taxa, documenting their survival in refugia located in the Mediterranean peninsulas of Iberia, Italy, and the Balkans, followed by postglacial expansion and colonization of northern Europe (Hewitt 1999; Tzedakis et al. 2013). In contrast to taxa restricted to areas with temperate climate, cold-adapted species occur in areas characterized by low summer and winter temperatures and short growing-season (e.g., alpine and arctic regions), but can display great variability in terms of tolerance to warmer temperatures, range size, and competition with other species (Birks 2008; Crawford 2008). The variable characteristics of cold-adapted species and their habitats have precluded the emergence of a unified consensus on their responses to Quaternary climatic shifts. Yet, in-depth understanding of how climatic cycles affect the processes that generate and erode the diversity of cold-adapted species is necessary to respond to the twin crises of global warming and biodiversity loss, which are especially severe in alpine and arctic regions (Engler et al. 2011; Dullinger et al. 2012).

In spite of the heterogeneity of cold-adapted species, only two main hypotheses have been proposed to explain their responses to Quaternary glacial cycles, and only one of those is supported by substantial evidence (Fig. 1). The first and most common hypothesis posits that cold-adapted species attained larger distributions during colder intervals (i.e., glacials) by surviving and spreading in climatically suitable peripheral and lowland ice-free regions (e.g., cold tundra and steppe plains beyond and below the ice margins). During interglacials, cold-adapted taxa retreated to refugia in colder parts of Europe, including northern regions and the summits of southern mountains (i.e., interglacial contraction hypothesis; Hewitt 2004; Stewart et al. 2010). The hypothesis of glacial expansions and interglacial contractions has been supported by several studies on alpine and arctic species (Kropf et al. 2003; Muster and Berendonk 2006; Dalén et al. 2007; Westergaard et al. 2010; Espíndola et al. 2012).

The alternative hypothesis proposes that some cold-adapted species may have attained larger ranges in warmer interglacial periods (e.g., Holocene) than during full glacial periods (Stewart et al. 2010).

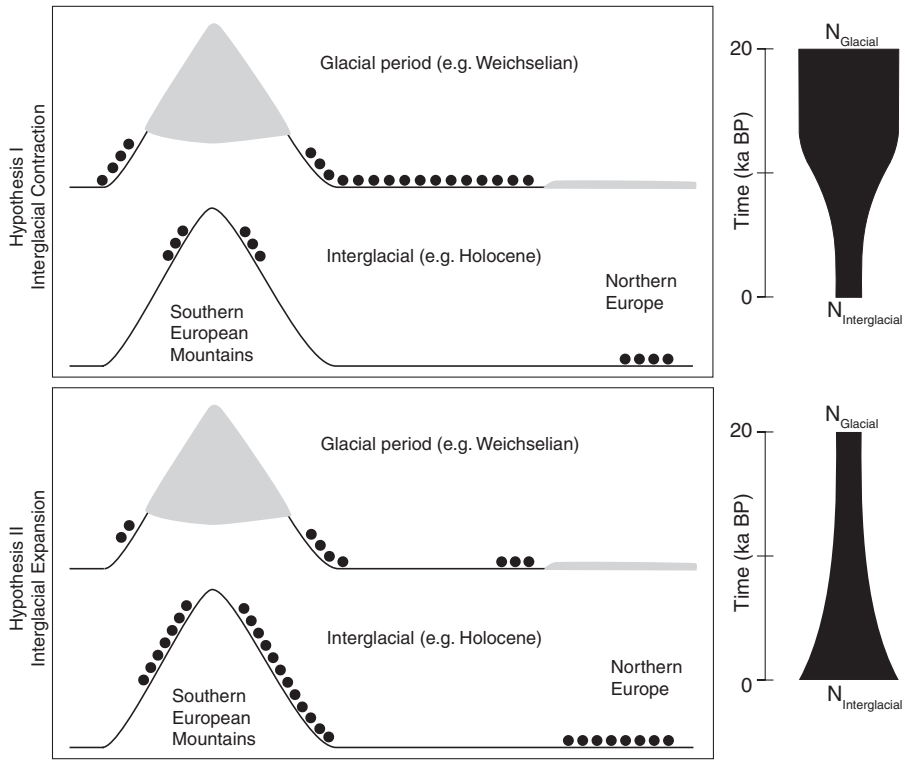

FIGURE 1. The two main, pre-existing hypotheses (left) and corresponding models of population-size changes (right) for responses of cold-adapted plants to Quaternary climatic oscillations in Europe. Hypothesis I: During colder intervals (i.e., Pleistocene glacials), cold-adapted species attained larger distributions by surviving and spreading in climatically suitable, peripheral and lowland ice-free regions, that is, cold tundra and steppe plains beyond and below the ice margins; during warmer intervals (i.e., Pleistocene interglacials and Holocene) they retreated into colder regions, including northern areas and summits of southern mountains (i.e., interglacial contraction). Hypothesis II: During colder intervals, cold-adapted species may not have been able to fully expand their ranges, due to low competitiveness and/or dryness of glacial steppes beyond the ice margins, becoming restricted to the proximity of glaciated regions; during interglacials they were able to persist in their previously occupied habitats and expand upwards and northwards into habitats newly made available by retreating glaciers (i.e., interglacial expansion). Ice sheets are shown in gray. Black filled circles represent species ranges. N_{Glacial} = species effective population size during glacial periods, $N_{\text{Interglacial}}$ = species effective population sizes during interglacial periods.

These species may have been unable to fully expand their ranges during colder intervals due to their low competitiveness and/or the dryness of glacial steppes beyond the ice margins, becoming restricted to the proximity of glaciated regions during glacials (Schmitt 2007). According to this hypothesis, some cold-adapted species, particularly plants with broader climatic tolerances, may have been able to persist in lowland, open habitats during glacial maxima, shifting, and gradually expanding their ranges upwards and northwards into habitats rendered available by retreating glaciers, where biotic competition was low, during interglacials (i.e., interglacial expansion hypothesis; Birks 2008; Stewart et al. 2010). This second hypothesis might better apply to species that currently exhibit a facultative alpine distribution (i.e., wide altitudinal and ecological range) in central European mountains, and a southern boreal distribution in northern Europe (Ronikier et al. 2008b). However, scarce evidence is available in support of the interglacial expansion hypothesis, in part because, to our knowledge, no explicit, empirical assessment of the two main alternative hypotheses on the responses of cold-adapted plant species to Late Quaternary glacial cycles has been conducted yet.

Reconstructing species responses to past episodes of climate change requires three main sources of evidence: phylogeographic patterns of genetic diversity, species distribution models (SDMs) through time, and/or the fossil record (rarely available at sufficient resolution in space and time). In this article, we exploit recent advances in the integration of the former two sources of evidence to elucidate the responses of a cold-adapted plant species to Quaternary climatic cycles. Phylogeography investigates the spatial arrangement of genetic lineages and their genealogical links by combining analytical principles used in population genetics and phylogenetics (Avise 2009; Hickerson et al. 2010). The recent advent of high-throughput sequencing is revolutionizing phylogeographic research, because it enables the analysis of thousands of genome-wide markers, allowing for increased resolution of genetic relatedness even among recently diverged populations (Emerson et al. 2010; Davey et al. 2011; Carstens et al. 2012;

Lemmon and Lemmon 2012; 2013). Furthermore, newly available paleoclimatic data sets at high spatial and temporal resolution now enable us to predict past species distributions and identify potential range expansions and contractions through time (Nogués-Bravo 2009; Svenning et al. 2011; Patsiou et al. 2014). Moreover, the suitability of climatic shifts as a proxy for historical demographic changes through the Late Quaternary has been recently demonstrated for a wide range of organisms (Hoareau 2015).

Phylogeographic and climatic data can be integrated in the framework of statistical phylogeography to inform and test alternative evolutionary hypotheses (Alvarado-Serrano and Knowles 2014). Statistical phylogeography enables the comparison of alternative phylogeographic scenarios by simulating patterns of genetic variation under complex evolutionary and demographic processes, allowing for the estimation of relevant model parameters (including timing of population divergence, population expansions, and migration) that could not be previously estimated using descriptive phylogeographic methods (Knowles 2009). This integrative framework thus provides a robust approach to explain current species distributions and genetic structure in relation to historical climate oscillations (Richards et al. 2007; Gavin et al. 2014).

Here, we use statistical phylogeography to explicitly evaluate the proposed contrasting hypotheses (Fig. 1). The selected species, *Primula farinosa* L., represents an ideal study system because it is adapted to cold, moist conditions at high altitudes and latitudes (Richards 2003); presents a broad, disjunct range in Europe that epitomizes the current fragmented distribution of cold-adapted species (Stewart et al. 2010; Fig. 2); and evolved during the Late Quaternary (de Vos et al. 2014). To estimate the time and extent of demographic contractions and expansions during the Late Quaternary, we project SDMs through time using a recently developed, high-resolution, paleoclimatic data set spanning the last 72 ka (Pleniglacial to Holocene; Maiorano et al. 2013; Schmatz et al. in revision). We also generate genome-wide sequence data using a Reduced Representation Library (RLL) approach to reconstruct the spatial structure, genetic diversity, and evolutionary relationships of genetic lineages within *P. farinosa*. Finally, by integrating the results of climatic and genomic analyses, we test five models (two under each of the alternative hypotheses and a null model) for the extent and direction of population-size changes in *P. farinosa* through the Late Quaternary. By adopting an Approximate Bayesian Computation (ABC) approach to evaluate pre-existing hypotheses on how cold-adapted species responded to past climatic cycles, namely, through either range expansion or contraction during warmer intervals (Fig. 1), the present study contributes new knowledge on the processes that shaped the distributions and diversity of cold-adapted species in the Late Quaternary.

Materials and Methods

Study System

Primula farinosa L. a cold-adapted species within the montane and high alpine flora of southern Europe (Carpathians, Alps, Pyrenees), where it occurs between 400 and 2900 m a.s.l. (Hambler and Dixon 2003; Richards 2003; Theodoridis et al. 2013). In northern Europe (British Isles, Baltic region, and Southern Scandinavia), *P. farinosa* occurs in flat areas between 0 and 400 m a.s.l. (Fig. 2; Hambler and Dixon 2003; Richards 2003; Theodoridis et al. 2013). It is an insect pollinated, short-lived perennial herb included in *Primula* sect. *Aleuritia* Duby subsect. *Aleuritia* (Primulaceae); it is diploid ($2n = 2x = 18$; Bruun 1932) and heterostylous, hence mostly outcrossing (Hambler and Dixon 2003; Richards 2003). The habitat of *P. farinosa* encompasses calcareous fens, edges of streams or lakes, and drier calcareous grasslands at high altitudes. Dormancy of *P. farinosa* appears to be enforced at the end of the growing season, and growth is resumed early in the year—typical characteristics of arctic and alpine perennials (Urbanska and Schutz 1986; Hambler and Dixon 2003). Previous analyses of its ecological characteristics established that this species has broader climatic preferences than those of its closest alpine/arctic relatives in sect. *Aleuritia* (Theodoridis et al. 2013). Molecular phylogenetic and morphological analyses concluded that *P. farinosa* played a central role in the Quaternary evolution of *Primula* sect. *Aleuritia*, likely contributing to the origin of polyploid species via secondary contact following glacial retreat (Hultgård 1990; Guggisberg et al. 2006, 2009; Theodoridis et al. 2013; de Vos et al. 2014).

Species Distribution Modeling

Species occurrences and environmental predictors.—Occurrences of *P. farinosa* were recorded during field surveys between 2011 and 2013. Additional georeferenced occurrences were obtained from the following global and national databases: GBIF (http://www.gbif.org), ANTHOS (Spain, http://www.anthos.es), the Data Center of the Swiss Flora (ZDSF, https://www.infoflora.ch/), and the French Alpine Botanical Conservatory (www.cbn-alpin.fr). The validity and accuracy of all sources were checked during field surveys by visiting multiple localities obtained from each source. Sampling points were spatially filtered and occurrences closer than 1 km to each other were removed, resulting in a final data set of 1764 occurrence points.

To select climatic predictors for SDM, we first extracted the current monthly mean temperature (tmean) and precipitation (prec) variables from the WorldClim data set (Hijmans et al. 2005) at 30-s (ca. 1 km) spatial resolution for the region considered in this study (Fig. 2). Using these monthly climatic values, we generated a set of 17 climatic

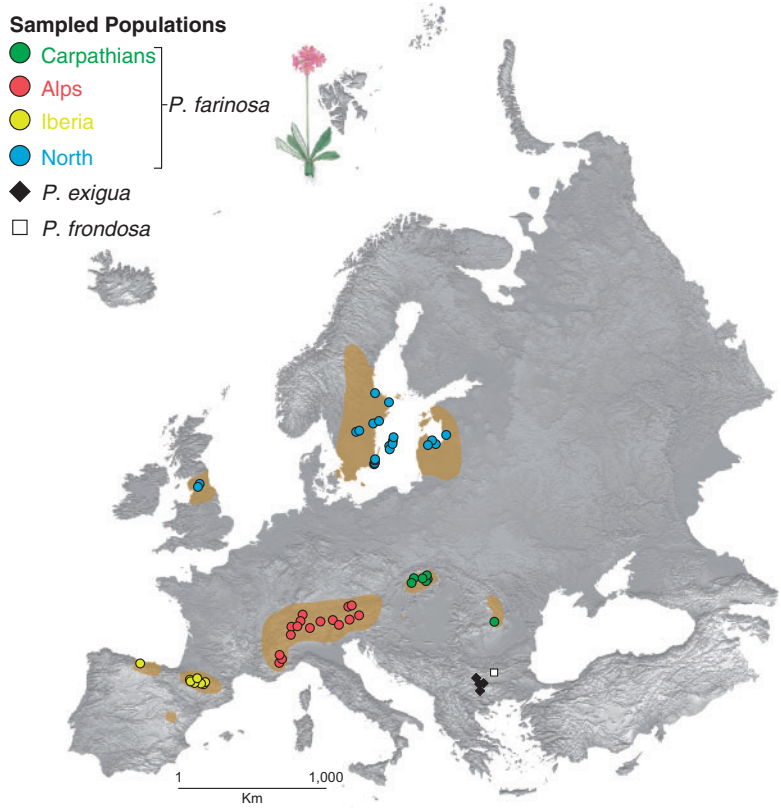

FIGURE 2. Sampling localities of P. farinosa, P. exigua, and P. frondosa populations across their ranges in Europe. Brown areas indicate the current known range of P. farinosa in Europe based on field observations and information drawn from national and international floras.

variables (Supplementary Table S2, available on Dryad at http://dx.doi.org/10.5061/dryad.1fp80) considered crucial in determining species boundaries, especially for large-scale geographic patterns (Wiens 2011) and cold-adapted plants (Körner 2003). We then evaluated the relevance of each variable for the ecological preferences of the study species using three different statistical techniques implemented in R (R Development Core Team 2013): generalized linear models (GLMs; McCullagh and Nelder 1989), generalized additive models (GAMs; Hastie and Tibshirani 1990), and random forest (RF; Breiman 2001). We retained the climatic variables that showed the highest independent contribution to variation in the three techniques mentioned above (Aguirre-Gutiérrez et al. 2013) and were not highly correlated with each other (Pearson correlation <0.7). The final set consisted of the following five variables: i) annual range of mean monthly temperature, ii) mean temperature of the coldest month, iii) mean temperature of the warmest month, iv) precipitation of the driest month, and v) precipitation of the wettest quarter. These Bioclim variables were used to project the potential distribution of *P. farinosa* under current and past climatic conditions.

To reconstruct the potential past distributions of *P. farinosa* and identify stages of expansion and contraction through time, we used geographic paleoclimatic layers of monthly mean temperature and precipitation data from Maiorano et al. (2013) and described in Singarayer and Valdes (2010). The available paleoclimatic layers span a period of 72 ka (from the onset of the cold period of the Würm/Weichselian glaciation to present time) at 1 ka intervals from 1 to 20 ka BP (last glacial maximum; LGM) and at 4 ka intervals from 21 to 72 ka BP. In order to match the spatial resolution of the Worldclim variables, the paleoclimatic data set was downscaled to 1 km using the delta method [see Patsiou et al. (2014) for more details on the downscaling procedure].

Calibration of SDMs.—We used a suite of five modeling techniques combined into an ensemble approach (as recommended in Guisan and Thuiller 2005; Araújo and New 2007) to reconstruct the current and past potential distribution of *P. farinosa*. GLMs, GAMs, generalized boosted models (Friedman 2001), and RF were implemented using custom scripts in R, while we used Maxent v.3.3.3 (Phillips et al. 2006) for maximum entropy models. These modeling techniques have been shown to display good transferability in space and time and to be among the best-performing techniques for predictive modeling (Elith et al. 2006; Randin et al. 2006; Howard et al. 2014). The number of pseudo-absences for each modeling technique was chosen based on the recommendations of Barbet-Massin et al. (2012; Supplementary Table S3, available on Dryad) and

calibration was repeated 10 times for each technique. We evaluated the predictive performance of each model by applying 10-fold cross-validation and using the area under the receiver operating characteristic curve (AUC; Fielding and Bell 1997) and the True Statistics Skills value (TSS; Allouche et al. 2006).

Spatial projections and distribution-through-time analysis.—SDMs for *P. farinosa* were projected onto current and past climates and the probabilities of occurrence obtained from those projections were transformed into binary presence/absence maps using the threshold that maximized the TSS (Liu et al. 2005). As in Patsiou et al. (2014), we combined all 10 replications of each modeling technique and considered a pixel as potentially suitable when at least 5 of the 10 model replications predicted the presence of *P. farinosa*. To assess uncertainty in the predictions and produce maps of potentially suitable surfaces for each time slice, we combined all SDM techniques into four possible ensembles of projections: (i) at least two techniques predicting suitable areas, defined as "minority"; (ii) at least three techniques predicting suitable areas, defined as "majority 3"; (iii) at least four techniques predicting suitable areas, defined as "majority 4"; and (iv) all five techniques predicting suitable areas, defined as "consensus". Additionally, we considered as unsuitable the areas covered by ice at each time slice (Ehlers et al. 2011; Supplementary Table S4, available on Dryad).

We used the four ensembles above to characterize expansion and contraction responses to climatic oscillations at different spatial and temporal scales. First, we counted the number of climatically suitable cells across the entire range of *P. farinosa* and across the available time slices from 72 ka BP to present. Second, we counted the number of climatically suitable cells within regions corresponding to lineages identified by the results of molecular analyses (see below) and across the time slices available for the current interglacial period (i.e., Holocene; 10 ka BP to present times). Each region was circumscribed as follows: we first defined circular buffers (each with a radius of 250 km) around each occurrence point within each region, then we calculated a convex hull around these buffers. The radius value was estimated by taking into account *Primula* dispersal rates (Brys and Jacquemyn 2009) and the maximum dispersal distance a herbaceous plant could have covered during the Holocene (Pakeman 2001). The results of the distribution-through-time analyses described above were then used as proxies for changes in population sizes within the statistical phylogeography framework (see "*Hypothesis Testing*").

Molecular Analyses

Sampling.—During springs of 2011, 2012, and 2013, we collected leaf tissue from 144 individuals of 53 populations (one to five individuals per population, see Supplementary Table S1, available on Dryad) that encompassed most of the known distribution of *P. farinosa*, were located at least 15 km apart from each other (Fig. 2), and covered both its ecological and geographic gradients (Albert et al. 2010). We also sampled 12 individuals of *P. exigua* Velen. and 1 individual of *P. frondosa* Janka, both endemic to the Balkan Peninsula and closely related to *P. farinosa* (Richards 2003; Guggisberg et al. 2006), to be used as outgroups in phylogenomic analyses.

nextRAD sequencing.—Collected leaf samples were preserved in silica gel and DNA was extracted using a modified CTAB protocol (Doyle and Doyle 1990). Samples were normalized to a total input of 10 ng genomic DNA per sample. Genotyping by sequencing, including library preparation and sequencing, was performed by SNPsaurus (SNPsaurus.com) using nextRAD libraries with the selective primer sequence GTGTAGAGC. The nextRAD library preparation protocol performs a complexity reduction of the genome by amplifying Nextera-tagmented DNA with a selective primer, so that DNA fragments with the reverse complement of the selective sequence at an end will be preferentially amplified. Single-end sequencing was carried out using two lanes of an Illumina HiSeq 2000 (University of Oregon High-throughput Sequencing Core), producing raw reads that were 101 bp long.

Bioinformatics.—We developed custom scripts written in python to process the original raw reads. Initial analysis of the raw reads indicated the existence of a few organellar loci with extremely high coverage and invariability among individuals. To exclude these chloroplast and mitochondrial DNA sequences from our raw data prior to downstream analyses, we used organellar genomes of the closest relatives of *Primula* because no complete organellar or nuclear genome sequences were available from the genus at the time of analysis. Raw reads were blasted against four chloroplast (*Ardisia polysticta*—Primulaceae, *Arbutus unedo*—Ericaceae, *Vaccinium macrocarpon*—Ericaceae, *Camellia oleifera*—Theaceae) and one mitochondrial (*Vaccinium macrocarpon*—Ericaceae) genomes of species included in Ericales by the Angiosperm Phylogeny Group III (http://www.mobot.org/MOBOT/research/APweb/). Reads with a BLASTN hit to the organellar genomes at e $<10^{-4}$ were discarded from the raw data, leaving only reads from the nuclear genome. For quality filtering and trimming of the raw nuclear reads, we removed reads that had less than two-thirds of the bases with Phred quality score (Q) $\geqslant$30 in the first half of the read and reads containing at least one uncalled base (Minoche et al. 2011); we then trimmed the last 11 bp of the reads, for they contained low quality bases in the majority of the samples.

Our final, filtered data set consisted of nuclear reads that were 90 bp long (Supplementary Table S6, available on Dryad). To identify putative homologous loci across samples, we employed the STACKS pipeline v.1.18

(Catchen et al. 2013) and applied the following parameter values: a minimum depth (coverage) of 20 identical reads per stack was required and stacks with coverage of more than two standard deviations above the mean were removed (Catchen et al. 2013); we allowed a maximum distance (*M*) between stacks of eight nucleotides and a maximum number of two stacks at a single *de novo* locus in each individual; 12 mismatches were allowed between putatively homologous loci (*n*) across all individuals. Although these settings may be relatively relaxed when assessing intraspecific genetic diversity, they are necessary to capture potential admixture and recover putative homologous loci among divergent lineages (Leaché et al. 2014; Lischer et al. 2014). To assess the influence of varying the alignment-mismatch thresholds, we performed additional analyses using an *M* value of four mismatches and an *n* value of six mismatches. Because results did not significantly differ between the different combinations of mismatch values (see Supplementary Fig. S3, available on Dryad), the results presented in main text are inferred by using the former values. The STACKS pipeline was run on two data sets: one that included only *P. farinosa* populations (i.e., "ingroup" data set) and one that included also the outgroup species *P. exigua* and *P. frondosa* (i.e., "full" data set). Putatively homologous loci present in at least two populations within each data set were kept for subsequent analyses. SNPs were called by aligning homologous loci across all individuals, including the alternative alleles for heterozygous loci as recovered by STACKS based on stacks of identical reads.

We ran a preliminary series of analyses of the genomic data set by applying a range of percentages (from 0% to 100%, at 10% intervals) for missing data per locus. As expected, increasing this percentage allowed for the inclusion of more loci in the matrix. The same phylogeographic structure (i.e., lineages corresponding to geographic areas) was consistently recovered for all values above 60% (see Appendix 1 for further details); hence, this threshold was used for downstream analyses. Because structured patterns (i.e., nonrandom distribution) of missing data across taxa could bias phylogeographic signal (Patterson et al. 2006; Rubin et al. 2012), we further investigated our data set for such patterns under the chosen threshold and developed a simple index to identify potential nonrandom distribution of missing data (Appendix 1).

Population structure and genomic diversity.—Population genomic analyses were performed on the "ingroup" data set. We first used the Bayesian clustering method implemented in STRUCTURE v.2.3.4 (Pritchard et al. 2000) to identify groups of individuals with similar allele-frequency profiles and obtain an estimate for the most likely number of ancestral gene pools. All analyses were run using the admixture model with correlated allele frequencies within populations and no a priori information on each individual's origin; each individual was represented as diploid, thus allowing for heterozygosity. Since STRUCTURE assumes that the investigated loci are unlinked, we ran it with only one random SNP per locus (total SNPs = 2055) and repeated this analysis 20 times to account for the stochasticity stemming from the random choice of one SNP per locus. We performed 10 replicate runs for each value of the number of ancestral gene pools, *K*, between 1 and 10. In each replicate, 100,000 Markov chain Monte Carlo iterations were run after a burn-in period of 50,000 iterations. Convergence of the Markov chain was ensured by checking the values of summary statistics (α, *F*, likelihood) across iterations and replicates (Pritchard et al. 2000). The most likely value of *K* was selected based on two criteria: (i) the *K* value at which the likelihood distribution began to plateau or decrease and (ii) second-order rate of change in values of *K* (ΔK) (Evanno et al. 2005). For the best *K* value, the results of the 20 randomly selected SNP repetitions and 10 replicated STRUCTURE runs per repetition were combined using the "greedy" algorithm within CLUMPP v1.1.2 (Jakobsson and Rosenberg 2007).

We then assessed genomic diversity in each of the four main genetic groups recovered by STRUCTURE (see the "Results" section). Although STRUCTURE is relatively robust to SNP ascertainment bias when using large multilocus data sets (Haasl and Payseur 2011), this bias is known to influence statistics that summarize genetic variation and differentiation across populations (Lachance and Tishkoff 2013; McTavish and Hillis 2015). Therefore, to assess the genomic diversity of the four genetic groups (referred to as lineages hereafter), we followed a haplotype-based approach that can partially correct for SNP ascertainment bias (Conrad et al. 2006; Browning and Weir 2010; Lachance and Tishkoff 2013). We thus used the full sequence of each locus as recovered in the STACKS analysis, including two sequences at heterozygous loci (François et al. 2008). We retained loci that were present in at least 10 individuals, resulting in a minimum of 20 sequences per locus and per lineage, and applied a rarefaction approach to account for differences in sample size within the lineages (Kalinowski 2004). For each of the four lineages, we calculated the expected allelic richness as the number of distinct alleles per locus and the expected private allelic richness as the number of alleles unique to the lineage (i.e., not found in other lineages). Both statistics were calculated for sequence sample sizes (g) from 2 to 20 (1–10 diploid individuals). This analysis was conducted using a custom program written in python; the script is available in the Dryad data submission for this manuscript (http://dx.doi.org/10.5061/dryad.1fp80).

Phylogenomic analyses.—To infer the evolutionary relationships among the sampled individuals of *P. farinosa*, phylogenomic analyses were performed on the "full" data set. A total of 2006 loci comprising 180,540 aligned nucleotide positions and 21,781 variable sites were thus concatenated to infer the *P. farinosa* tree. All heterozygous positions in each individual

were replaced by IUPAC ambiguity codes. Maximum-likelihood trees were estimated using RAxML v.8.0.2 (Stamatakis 2014) and rooted with the outgroup taxa *P. exigua* and *P. frondosa*. The rapid bootstrap algorithm (Stamatakis et al. 2008) with 1000 replicates was used to assess uncertainty in topology estimation. We also investigated the influence of heterozygosity on phylogenomic reconstruction by randomly selecting one of the two alleles (full sequences) at each heterozygous locus to generate haploid sequences for each individual and inferring an ML tree from the random haplotypes (Lischer et al. 2014), repeating the process of haplotype generation and tree inference 1000 times. For both approaches (IUPAC codes and random allele selection), we employed a super matrix constructed by concatenating all loci and performed a partitioned analysis by using an independent general time-reversible model of substitutions and variation in substitutions rates among sites assigned to each locus. A 50% majority rule consensus of the trees inferred from the two approaches was computed with SumTrees in the DendroPy package (Sukumaran and Holder 2010).

Phylogenomic methods that concatenate data across multiple loci may fail to resolve evolutionary relationships among recently diverged lineages due to the inherent stochasticity of the coalescent process across loci (Edwards et al. 2007). Therefore, the lineage tree was also inferred using two additional approaches, namely SNAPP (Bryant et al. 2012) and TreeMix (Pickrell and Pritchard 2012). By using the coalescent approach, SNAPP analyses allowed us to both reconstruct the order of divergence among lineages of *P. farinosa* and estimate the relative population sizes of the four main lineages identified by the population structure and phylogenomic analyses of the concatenated data set described above (see the "Results" section). Because SNAPP infers the lineage tree from unlinked, biallelic markers, we excluded all SNPs with more than two nucleotide states across populations and further reduced our data set to one random SNP per locus. Furthermore, in order to make our analyses computationally feasible, we reduced each population to one individual by selecting the individuals with the highest number of sequenced loci. The final data set consisted of 53 individuals (106 haplotypes) and 2105 randomly chosen SNPs. We applied a gamma prior for θ ($\alpha = 1$, $\beta = 200$) and uniform hyperprior for speciation rate λ in the Yule model. SNAPP was run until the effective sample size (ESS) values were greater than 200 after sampling every 1000 generations and discarding the first 10% of the samples as burn-in. ESS values and likelihood plots were visualized in Tracer v.1.6 (Rambaut et al. 2014). The analysis was repeated three times, each time choosing a new random SNP per locus and the complete tree sets were visualized using DensiTree (Bouckaert 2010). We then used TreeAnnotator v.1.8 (Rambaut and Drummond 2008) to determine the Maximum Clade Credibility tree and posterior probability values for each repetition.

TABLE 1. Characteristics and posterior probabilities of the five demographic models tested in the statistical phylogeography framework

Hypothesis	Model	Number of sampled parameters	Posterior probability	
			Standard rejection	Logistic regression
Expansion	Species-wide	15	0.72	0.76
	Lineage-specific	15	0	0
Contraction	Species-wide	15	0.05	0.08
	Lineage-specific	15	0	0
	Null	7	0.23	0.16

Notes: In the species-wide models, values for the Holocene growth rates for each lineage were drawn from a single prior distribution, while for the lineage-specific models these values were drawn from prior distributions specific for each lineage. Posterior probabilities were estimated using two approaches: the standard rejection approach by Pritchard et al. (1999) and the weighted multinomial logistic regression by Beaumont (2008).

To further validate the lineage tree inferred with SNAPP, we used TreeMix to estimate the maximumlikelihood tree for the lineages identified by the population structure and phylogenomic analyses of the concatenated data set. TreeMix uses as input a set of population allele frequencies and assumes biallelic, unlinked sites (Pickrell and Pritchard 2012). Therefore, we followed a similar approach as in SNAPP analysis, that is, we retained only one randomly chosen SNP per locus and excluded SNPs with more than two nucleotide states across populations. The analysis was performed on the "full" data set with the outgroups (*P. exigua* and *P. frondosa*) combined into one population. The analysis was repeated 20 times, each time choosing a random SNP per locus (the total SNP number varied between 1777 and 1808 across repetitions), and for each SNP repetition we ran 100 bootstrap replicates. A 50% majority rule consensus of the trees across all SNP repetitions and bootstrap replicates was computed with SumTrees.

Hypothesis Testing

We evaluated the two alternative hypotheses (i.e., interglacial contraction vs. expansion) on the responses of cold-adapted species to Late Quaternary glaciations in a statistical phylogeography framework by integrating genomic data with the results of SDMs. For each of the two hypotheses, we tested two distinct models that differed with regard to lineage growth rates during the Holocene (see Table 1). In one model, we used a single prior distribution (referred to as "species-wide" model hereafter) to draw values for each lineage's growth rates, which were inferred from the cell counts of SDMs across the entire range of *P. farinosa* through time. In the other model, we used different, lineage-specific prior distributions (referred to as "lineage-specific" model hereafter) inferred from region-specific cell counts of SDMs through time (see the "Spatial projections and distribution-through-time

TABLE 2. Priors, point estimates (mode of posterior distribution), and 95% HPD interval of demographic parameters and mutation rates under the species-wide interglacial expansion model

Parameter		Interglacial expansion model (species-wide)	
		Priors	Estimated values [95% HPD interval]
Growth rates ($\times 10^{-4}$)[a]	r_{A1}	−13 : −5	−10.27 [−10.72: −9.84]
	r_{A2}	5: 11	6.57 [4.89: 7.19]
	r_{C1}	−13 : −5	−6.49 [−6.88: −5.59]
	r_{C2}	5: 11	7.24 [6.0: 7.81]
	r_{i1}	−13 : −5	−7.69 [−8.11: −7.24]
	r_{i2}	5: 11	8.13 [7.71: 8.69]
	r_{N1}	−13 : −5	−8.22 [−8.94: −6.61]
Population size	N_{A1}	—	330,000
	N_{A2}	*	42,313
	N_{A3}	(0.5: 2) $\times N_{A2}$	0.96 [0.84: 1.22]
	N_{A4}	*	116,218
	N_{C1}	—	125,000
	N_{C2}	*	34,135
	N_{C3}	*	108,714
	N_{I1}	—	95,000
	N_{I2}	*	20,407
	N_{I3}	*	74,939
	N_{N1}	—	135,000
	N_{N2}	*	26,082
Time (ka BP)[b]	T_1	—	10
	T_2	16: 28	24.58 [23.67: 27.22]
	T_3	16: 55	42.31 [39.97: 44.61]
	T_4	—	64
	T_5	—	72
	T_6	55: 80	77.5 [75.82: 79.15]
	T_7	80: 200	87.91 [82.73: 112.3]
Migration rate[c]	m_{AI}	0.01: 0.5	0.0297 [0.010: 0.0831]
	m_{IA}	0.01: 0.5	0.0479 [0.0141: 0.1131]
Mutation rate ($\times 10^{-8}$)[d]	μ	0.1: 25	5.28 [4.76: 5.65]

Notes: Symbols correspond to those of Figure 7. A, Alps; C, Carpathians; I, Iberia; N, North; r, growth rate in the exponential function; N, population sizes; T, time of the evolutionary event; m, migration rate; μ, mutation rate. The interglacial contraction model differed from the interglacial expansion model in the growth rate priors (additive inverse of the minimum and maximum values).

[a]Negative growth implies population expansion.

[b]Assuming a generation time of 5 years.

[c]Migration between Alpine and Iberian lineages expressed as percentage of the source population size per generation.

[d]Per site per generation.

*Population sizes defined by the growth rates. If the current population size is N_0, and the growth rate is r, then the population size t generations ago is given by $N_t = N_0 \times e^{rt}$.

analysis" section). We additionally included a null model with constant population sizes through time to account for potential range shifts without demographic changes (Table 1). To estimate the posterior probabilities of the five models and the parameters of the model selected from the best fit between observed and simulated genomic data, we used ABC (Beaumont 2010; Csilléry et al. 2010; Wegmann and Excoffier 2010).

We briefly outline below the ABC procedure [see also Ray et al. 2010; Wegmann et al. 2010; Cornuet et al. 2014; Patiño et al. 2015 for details on implementation]. We used the program fastsimcoal v. 2.5.0.2 (Excoffier et al. 2013) to perform 10^6 coalescent simulations of genomic diversity under each of the five models for the Quaternary biogeographic history of *P. farinosa*. The model parameters were either fixed across all simulations and models (i.e., lineage tree topology, current population sizes) or randomly drawn from uniform prior distributions (i.e., growth rates, divergence times, migration times and rates, mutation rates; Table 2). Fixed parameters and prior distributions of parameters for each model were informed by the results of SDM and molecular analyses, and by information drawn from published studies, as detailed below:

i) Four main lineages were defined for the ABC analyses from the results of the STRUCTURE and phylogenomic analyses of the concatenated data set.

ii) The time frame for the splits among the four lineages of *P. farinosa* was defined as follows. The prior distribution for the Late Quaternary age of the most recent common ancestor of all four

lineages was informed by the results of published molecular dating analyses (de Vos et al. 2014; see Table 2). The order of lineage splits was inferred from the trees estimated with SNAPP and TreeMix (see the "Results" section). Strong intraspecific lineage differentiation is commonly interpreted as pre-LGM diversification in phylogeographic studies [see Schönswetter et al. 2005 for a review], thus the results of our molecular analyses (see above and in the "Results" section) justified a pre-Holocene prior distribution for the age of the most recent split in our models. Divergence times for all splits were sampled from uniform prior distributions (Table 2). Time was expressed in number of generations by assuming an average generation time of 5 years (personal observation).

iii) Effective population sizes (N) of extant lineages (Table 2) were inferred from relative sizes estimated by SNAPP analysis and converted to absolute values by reference to population sizes of other short-lived perennial plants (Gossmann et al. 2010).

iv) Time intervals of demographic expansions and contractions were bracketed by transition time points (treated as fixed parameters in the models) inferred via visually identifying changes in the number of suitable cells predicted by the models of the distribution-through-time analysis. We thus identified three time intervals with different demographic trends (see the "Results" section).

v) Prior distributions for population growth rates were calculated from changes in the counts of climatically suitable cells of SDMs at the beginning and the end of each time interval during which a demographic change was detected (see the "Results" section). The bounds (r) of the prior distributions for growth rates were obtained using the formula of Excoffier et al. (2013), which assumes exponential population growth

$$r = \frac{\log \frac{N_t}{N_0}}{t}.$$

where N_0 and N_t are the population sizes, expressed in number of suitable cells, at the beginning and at the end of each time interval, respectively. Negative and positive growth rates imply population contraction and expansion, respectively, backwards in time.

For the interglacial expansion models (both lineage-specific and species-wide), we estimated the lower and upper bounds of the prior distributions of growth rates for each time interval as follows. The lower bound was inferred from the model ensemble that showed the smallest change of climatically suitable cells during the interval; hence, N_0 and N_t were obtained from a single SDM ensemble for each interval. On the other hand, to account for SDM uncertainty, the upper bounds were inferred by calculating the change of climatically suitable cells between the minority and the consensus SDM ensembles (i.e., N_0 and N_t were obtained from the two extreme SDM ensembles). For the interglacial contraction models, growth-rate priors were defined by using the additive inverse of lower and upper bounds of the interglacial expansion models. Growth rates were sampled from uniform priors for both expansion and contraction models.

vi) Connectivity providing opportunity for migration between lineages was inferred from the paleodistribution maps. Migration was also inferred from the results of phylogenomic analysis of the concatenated data set using random allele selection, where closely related populations of a lineage appeared paraphyletic, probably due to introgression with another lineage (Eaton and Ree 2013; see the "Results" section). Migration rates and times were sampled from uniform distributions provided in Table 2.

vii) Mutation rates were sampled from a uniform distribution with a lower bound of 0.05×10^{-8} and an upper bound of 5×10^{-8} substitutions/site/year, based on previously published estimates for Primulaceae and other annual and perennial plants (Zhang et al. 2001; Gossmann et al. 2010).

For each of the 5×10^6 parameter value combinations (10^6 for each model), we simulated 1424 independent diploid loci of 90 bp length in all 144 individuals used in our study, maintaining the same size of the empirical data set that was used to estimate the genomic diversity of *P. farinosa* (see the "Population structure and genomic diversity" section). For each simulated locus, we randomly introduced the same amount of missing genotypes in each lineage as in our observed data set (Cornuet et al. 2014).

For each simulated data set, we calculated the same two summary statistics used in the genomic diversity analysis of the empirical data set: expected allelic richness and private allelic richness for each of the four main lineages (as in François et al. 2008), for a fixed sample size of 10 diploid individuals (20 sequences) as point estimate. We chose these two statistics because they explicitly account for different sample sizes among lineages. Additionally, commonly used summary statistics of genetic diversity (i.e., F_{ST}, θw, and π) calculated from genomic data generated by RRLs are known to deviate considerably from real values due to missing haplotypes, so they are inappropriate for demographic inferences (Arnold et al. 2013).

To estimate the posterior probabilities of the five tested models (i.e., the fit between observed and simulated data under each model), we first calculated the Euclidean distance between the observed and simulated

summary statistics (standardized across all simulations for each model), following Beaumont et al. (2002). We subsequently followed two approaches. The first approach is a standard rejection procedure proposed by Pritchard et al. (1999). For each of the five models, we retained the 5000 simulations with the smallest Euclidean distances to the observed summary statistics. The retained simulations for each model were combined and the final 25,000 simulations were ordered by ascending Euclidean distances recomputed on summary statistics standardized with common mean and standard deviation (Ray et al. 2010; Patiño et al. 2015). The posterior probability of each model was then computed as the proportion of simulations executed under the respective model that were included in the set of 1000 top simulations with the smallest distances (Estoup et al. 2004; Miller et al. 2005). The second approach, proposed by Beaumont (2008), uses a weighted multinomial logistic regression procedure to compute the posterior probability for each model. For each model, we used again the 5000 simulations closest to the observed data and the R package "abc" (Csilléry et al. 2012).

Given the uncertainty associated with the choice of certain demographic parameters (e.g., divergence times), we further evaluated the fit of the model with the highest posterior probability to the observed data. We computed the likelihood of the observed data under a postsampling regression adjustment (ABC–GLM; Leuenberger and Wegmann 2010) and compared it with the likelihood of the 1000 retained data sets (simulations with the smallest distance to the observed data set under the respective model) using ABCestimator (Wegmann et al. 2010). The reported *P* value represents the fraction of the retained simulations with a smaller or equal likelihood (Wegmann et al. 2010).

To estimate the parameters of the model with the higher posterior probability, we used the general linear model postsampling regression adjustment approach implemented in ABCestimator (ABC–GLM; Leuenberger and Wegmann 2010). The ABC–GLM approach aims at establishing a simple statistical model among used model parameters and summary statistics. Because this model is known to fit well locally around the observed data (Leuenberger and Wegmann 2010), postsampling adjustment and parameter estimation was carried out using the 1000 top simulations. We report the mode of the posterior distribution and the 95% highest posterior density (HPD) interval for each parameter.

Results

Species Distribution Modeling

All five SDM techniques showed very good performance, with average AUC values ranging between 0.9224 and 0.9945 (values higher than 0.9 indicate excellent performance in terms of true positive rates; Pearce and Ferrier 2000) and TSS values between 0.786 and 0.9502 (values higher than 0.6 indicate strong agreement between the training and the validation data; Landis and Koch 1977; Supplementary Table S3, available on Dryad), reflecting appropriate selection of climatic variables. In addition to the observed distribution of *P. farinosa* in Europe, the predicted distribution also included regions where the species occurred in the past, but now is extinct or nearly extinct (e.g., Denmark, Poland, Ukraine, Croatia, Scotland; Fig. 3; see the "Discussion" section) and regions where close relatives occur (e.g., *P. exigua* in Balkan peninsula and *P. scandinavica* in Norway).

Ensemble projections of SDMs into past climates consistently predicted climatically suitable regions for *P. farinosa* that overlap with areas included in the current distribution of the species: the southwestern Alps, Iberia (Pyrenees, Cantabria), the British Isles, and a large part of France, including the Massif Central (Supplementary Fig. S1, available on Dryad). Scandinavia, where the species currently occurs, was predicted as suitable only after the LGM and mainly during the Holocene, after the peninsula became ice-free (Fig. 3; Supplementary Fig. S1, available on Dryad).

In the distribution-through-time analysis across the entire range of *P. farinosa*, the four ensemble projections (i.e., Minority, Majority 3, Majority 4, and Consensus) showed similar patterns of predicted range expansions and contractions across the last 72 ka, even though the specific numbers of predicted suitable cells through time varied among them (Supplementary Table S5, available on Dryad; Fig. 7a). Projections-through-time predicted an initial range contraction during the middle stages of the last glacial period in Europe (72–64 ka BP), then a relatively stable range until the end of the glaciations about 10 ka BP, followed by continuous range expansion during the Holocene (10 ka BP to present times).

The region-specific distribution-through-time analysis showed differential predicted range expansions (expressed in increases in the number of climatically suitable cells) within each region during the Holocene (Supplementary Fig. S2, available on Dryad). Range expansion was particularly pronounced in the Carpathians, followed by the Alps and Northern Europe. Range expansion was less pronounced in Iberia, where only the minority and consensus ensembles showed a relatively distinct increase in number of suitable cells (Supplementary Fig. S2, available on Dryad).

Molecular Analyses

Attributes of nextRAD data.—We obtained a total of 327,689,814 raw, single-end Illumina reads of 101 bp length. After removing the reads identified as organellar DNA, trimming and quality-control filtering, we retained a total of 208,064,697 reads of 90 bp length (Supplementary Table S6, available on Dryad) that were used in subsequent STACKS analysis. STACKS pipeline identified 17,595 loci for the full data set and 16,009 loci for the ingroup data set shared in at least two populations for each data set. A total of 154,990 SNPs were called in

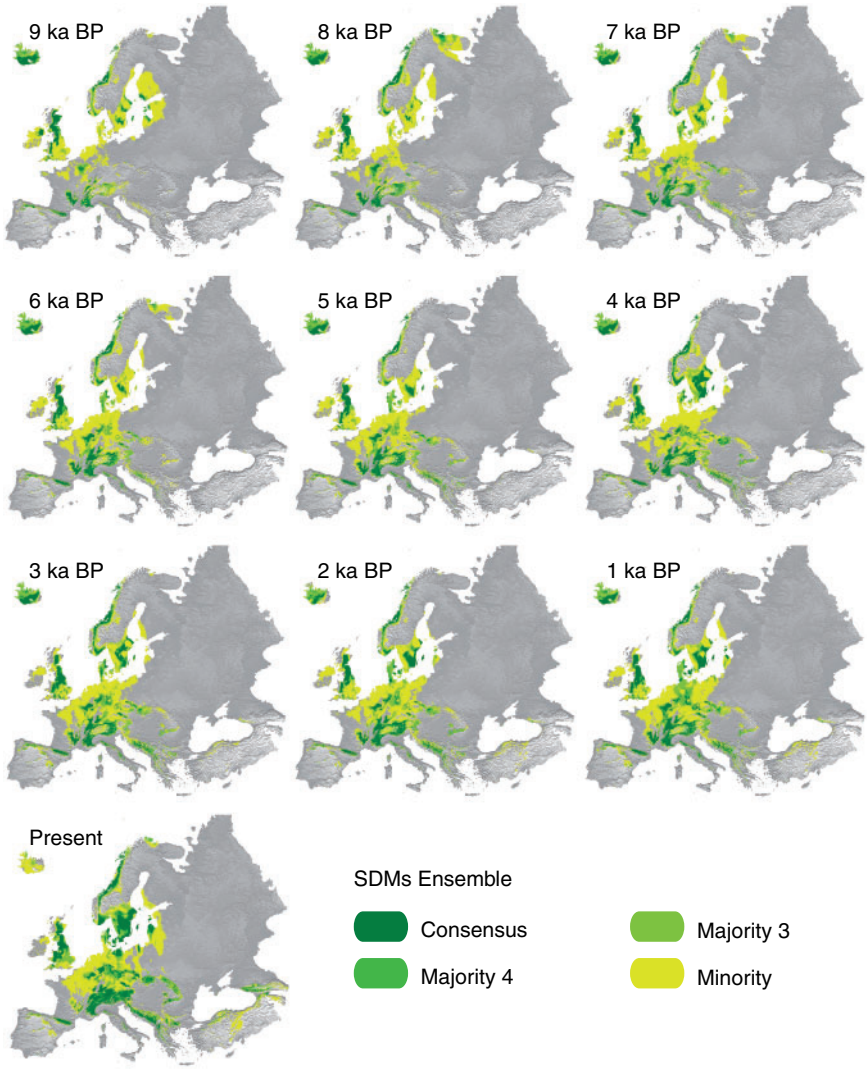

FIGURE 3. Climatically suitable regions for the distribution of *P. farinosa* through the Holocene. Colors correspond to the number of models (SDMs ensemble) that predict the respective grid cells as suitable.

the full data set and 136,019 SNPs in the ingroup data set.

Using a 60% threshold of missing data per locus (see above), we obtained a relatively equal ratio of missing genotypes across the four lineages of *P. farinosa*. This threshold resulted in a total of 37% missing data for the ingroup data set and 38.4% for the full data set (see Appendix 1), and was further used for all subsequent STRUCTURE and phylogenomic analyses.

Population structure.—For the majority of the 20 repetitions, STRUCTURE assigned all populations to four groups ($K = 4$), corresponding to the four main geographic areas (Fig. 4a). Specifically, based on our first criterion (i.e., likelihood distribution begins to plateau or decrease), 19 STRUCTURE runs supported four distinct groups and only one supported two. Based on our second criterion (ΔK), 15 runs supported four groups, whereas 5 supported K values between 2 and 9.

Population genomic diversity.—We obtained estimates of the mean number of distinct alleles (i.e., allelic richness) and the mean number of private alleles (i.e., private allelic richness) across the four lineages for subsamples of 2–20 sequences (10 diploid individuals) and 1424 loci (Fig. 4b). Alpine populations had on average the highest allelic richness across most investigated sample sizes, followed by the Northern populations, the Carpathian populations, and finally the Iberian populations. Carpathian populations had the highest number of private alleles per locus followed by the Alpine, the Iberian, and the Northern populations.

Phylogenomics.—Both phylogenomic approaches for handling heterozygosity (IUPAC encoding vs. random choice of alleles) produced similar, but not identical

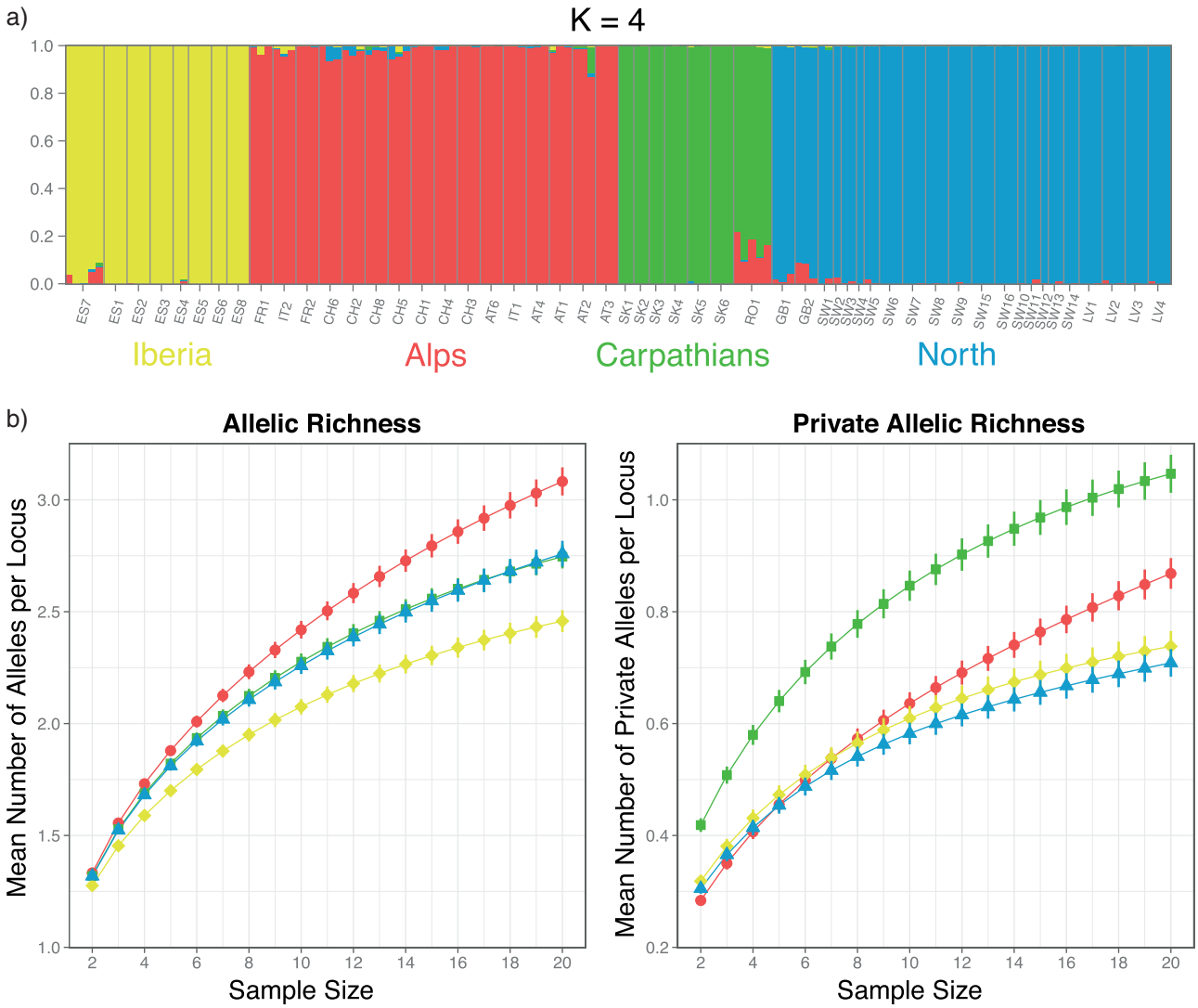

FIGURE 4. Population genomic analyses: a) Genetic structure of *P. farinosa* according to STRUCTURE analysis using one SNP per locus (total SNPs = 2055); b) Allelic richness (mean number of alleles per locus) and private allelic richness (mean number of private alleles per locus) of the four main lineages of *P. farinosa* as functions of sample size (i.e., rarefaction approach; Kalinowski 2004). Vertical bars show standard error.

topologies (Fig. 5). The Carpathian, Iberian, and Northern populations formed three monophyletic groups, consistent with STRUCTURE results, with the Northern lineage receiving lower statistical support under the IUPAC method (58.9%; Fig 5a). The Alpine populations formed an unresolved polytomy with the Northern and Iberian populations in the IUPAC approach. Under the random allele-choice approach, the Alpine populations were paraphyletic, for the southwestern Alpine samples formed a clade that was more closely related to the Iberian clade than to the rest of the samples from the Alps, with 89.4% of the trees supporting the respective clade (Fig. 5b).

TreeMix and SNAPP analyses resulted in identical tree topologies. Specifically, all three replications in the SNAPP lineage-tree analyses yielded the same well-supported topology (posterior probability of all nodes = 1; Fig. 6a), with an initial divergence between the Carpathian and the rest of the European lineages, followed by a divergence of the Iberian from other West-European lineages, and finally a divergence between the Alpine and the Northern lineages. All runs converged after 3–4 million generations. When using different priors in trees with few internal nodes, SNAPP is expected to produce unstable estimates of parameter θ (i.e., the product of mutation rates and effective population sizes; Rheindt et al. 2014), hence of effective population sizes. In our analyses, while the relative θ between lineages remained the same when using different priors, the absolute θ varied greatly. Therefore, we relied on relative population sizes across the four lineages derived from SNAPP analysis for the coalescent-based simulations (Supplementary Table S7, available on Dryad). The results of TreeMix analyses are illustrated in Figure 6b. The majority of maximum-likelihood trees across all SNP repetitions and bootstrap replicates

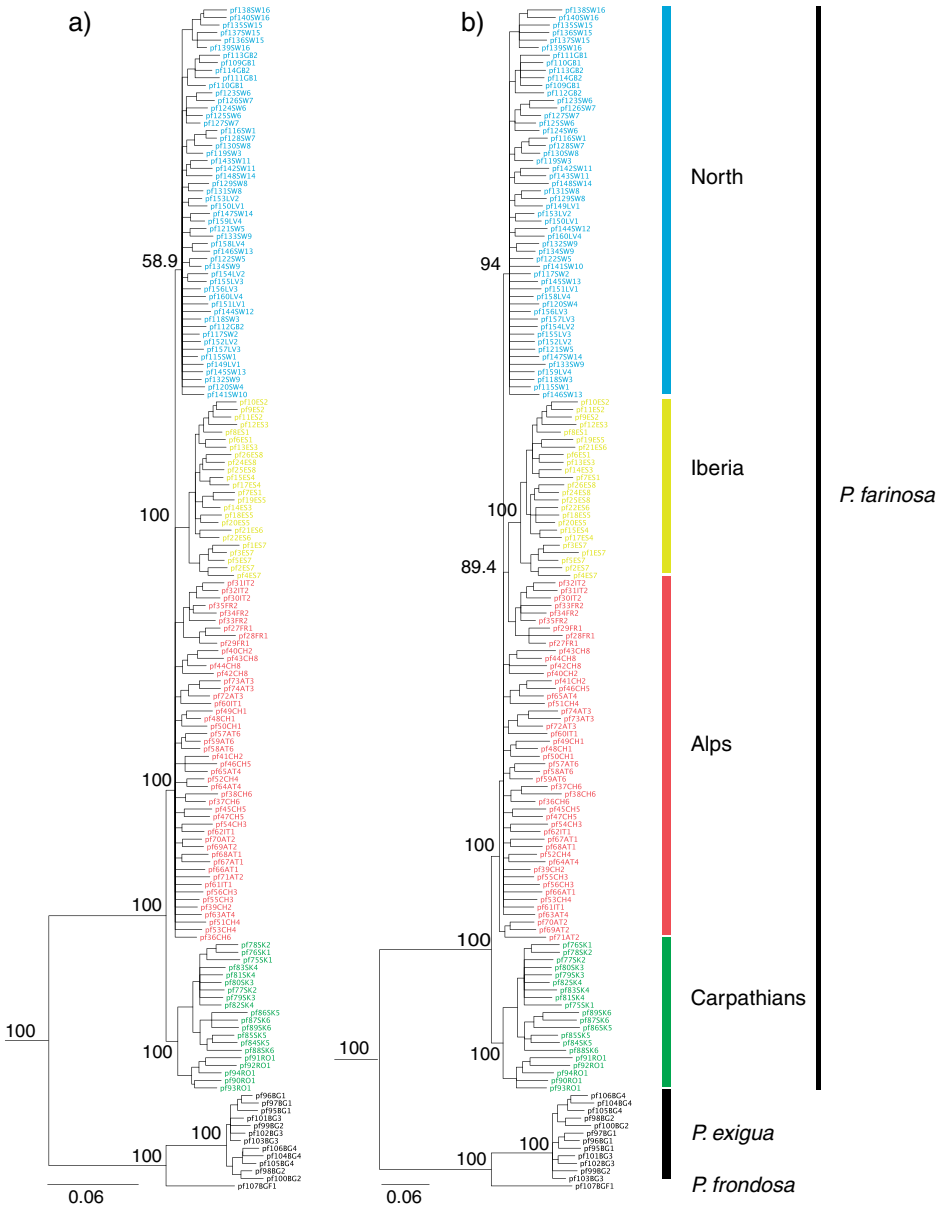

FIGURE 5. Phylogenomic analyses: Maximum-likelihood trees from 2006 loci, comprising 180,540 aligned and 21,781 variable positions. Terminals represent haplotypes obtained with two different approaches for handling heterozygosity: a) All heterozygous SNP positions in each individual were replaced with IUPAC ambiguity codes; statistical support was estimated from 1000 bootstrap replicates; b) Haploid sequences were generated for each individual by randomly selecting one of the two alleles at each heterozygous locus; statistical support was obtained by repeating the haplotype-generation process 1000 times. Both trees were rooted using the two outgroup species, *P. exigua* and *P. frondosa*. Note that the scale of branch lengths differs between the two trees.

supported the same topology, with support values ranging from 0.94 to 1.

Hypotheses Testing

The results of the independent molecular and SDM analyses were incorporated in the five demographic models as follows (see also the "Hypotheses testing" section in Materials and Methods). For the interglacial expansion models, we assumed size contraction starting at 72 ka BP (at the onset of Mid-Glacial) and lasting until 64 ka BP, size expansion starting at the onset of Holocene (10 ka BP) and lasting until present times as indicated by the distribution-through-time analysis (Fig. 7a), and stable linage population sizes between the two time intervals. These time intervals were inferred from the distribution-through-time analysis. For the interglacial contraction models, we assumed size expansion between 72 and 64 ka BP and size contraction starting at 10 ka BP until present times. These demographic transitions closely resemble the two-epoch demographic model

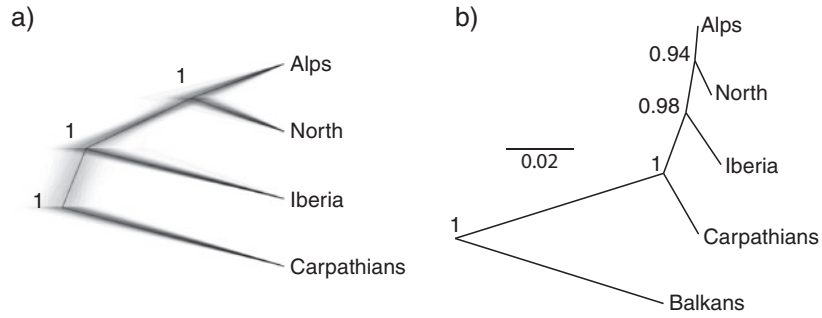

FIGURE 6. SNAPP and TreeMix analyses: a) Lineage tree obtained by SNAPP analysis of 53 individuals and 2105 SNPs (one SNP per locus); posterior probability values are shown at each node; b) Maximum-likelihood tree obtained by TreeMix analysis. Numbers at each node represent bootstrap support values across all SNP repetitions (20) and bootstrap replicates (100). The total SNP number varied between 1777 and 1808 across SNP repetitions. The individuals of P. exigua and P. frondosa were grouped together ("Balkans" lineage) and used as outgroup.

with exponential population growth (Shapiro et al. 2004; Crandall et al. 2012). The values used to inform the exponential growth rates for the species-wide models are shown in Figure 7a and in Supplementary Table S5, available on Dryad, while the ones used to inform the growth rates for the lineage-specific models are shown in Supplementary Figure S2, available on Dryad.

We assumed migration between the Alpine and Iberian lineages during LGM, as indicated by the connectivity of the two regions in the paleodistribution maps (Fig. 7 map inset; Supplementary Fig. S1, available on Dryad) and by relatedness between the southwestern Alps and Iberia revealed in the phylogenomic analyses (Fig. 5b).

Both model-choice procedures provided strong support for the species-wide interglacial expansion model, with 0.72 and 0.76 posterior probabilities under the standard rejection and the weighted multinomial logistic regression procedure, respectively (Table 1). The second best model was the null model (no population size changes), with 0.23 and 0.16 under the standard rejection and the weighted multinomial logistic regression procedure, respectively. Additionally, the species-wide contraction model received very low support (0.05 and 0.08 posterior probabilities). The lineage-specific models received no support by the two model-choice procedures. The estimated P value produced by ABCestimator was 0.09, indicating a good fit of the species-wide interglacial expansion model to the observed data. Therefore, we will mostly refer to the results of the species-wide interglacial expansion model in the "Discussion" section.

The demographic parameter estimates under the species-wide interglacial expansion model are provided in Table 2 and in Figure 7b. The split between the Carpathian and the rest of the European lineages was estimated at 87.91 ka BP (82.73–112.3 ka BP 95% HPD), between the Iberian and the western European lineages at 77.5 ka BP (75.82–79.15 ka BP 95% HPD), and between the Alpine and the Northern lineages at 42.31 ka BP (39.97–44.61 ka BP 95% HPD). The estimated contraction rates during the early stages of the Mid-Glacial period (72–64 ka BP) and expansion rates during the Holocene (10 ka BP to present times) are provided in Table 2. The estimated migration time between the Alpine and the Iberian lineage was 24.58 ka BP (23.67–27.22 ka BP 95% HPD). The migration rates (as percentage of the source population size per generation) from the Alpine to Iberian lineage and vice versa were 0.0297 (0.010–0.0831 95% HPD) and 0.0479 (0.0141–0.1131 95% HPD), respectively.

DISCUSSION

In this study, we investigated the effects of Late Quaternary climatic fluctuations on the range dynamics of the cold-adapted plant *P. farinosa*. The combination of recent methodological advances, both experimental (generation of large amounts of genomic data) and analytical (explicit modeling of demographic variables), with newly published data (high-resolution paleoclimatic layers) allowed us to explicitly test contrasting hypotheses (interglacial contraction vs. interglacial expansion) on the response of cold-adapted species to past climatic cycles. The present study thus demonstrates the potential of integrating genomic and climatic data into a rigorous hypothesis-testing approach to discriminate between alternative demographic models. Our results provide the first empirical evidence for interglacial demographic expansion of a cold-adapted plant during the Late Quaternary, implying that such species need not necessarily respond to warming trends by contracting their range, as suggested in previous studies.

First Empirical Evidence for Interglacial Range Expansion in a Cold-Adapted Species

The statistical phylogeographic approach used in our study provided strong support for the species-wide interglacial expansion of *P. farinosa* (Fig. 7) and much lower support for the null model of constant population sizes and for the species-wide interglacial contraction model (Table 1). Moreover, models in which

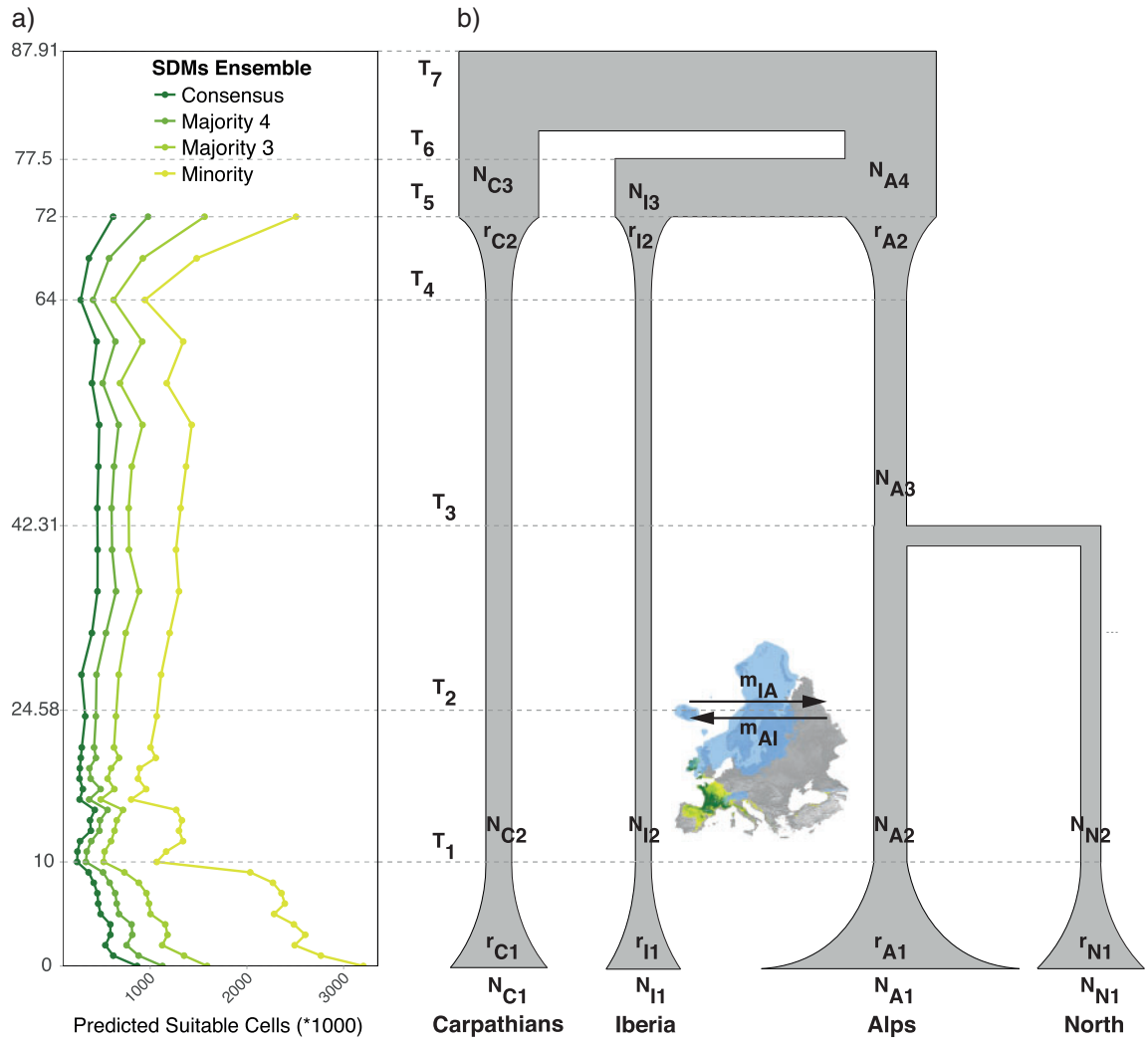

FIGURE 7. Overview of the interglacial expansion model for cold-adapted species (see Fig. 1) supported by statistical phylogeographic analyses of *P. farinosa*: a) Number of predicted suitable pixels through time inferred from SDM ensembles, with example of paleodistribution at 24 ka BP in inset map; b) The species-wide interglacial expansion model for the spatiotemporal evolution of *P. farinosa* informed by the order of lineage splitting in Figure 6 and predicted demographic fluctuations in a). The Carpathian lineage split first, followed by the Iberian lineage and by the final divergence between Alpine and Northern lineages. Estimated times (modes of posterior distributions) of lineage splitting, demographic transitions, and migration are indicated by gray dashed lines (T_1 to T_7). We assumed bidirectional migration between the Alpine and the Iberian lineage during the LGM (estimated migration time at 25.58 ka bp), when the species range likely extended between the Alps and Iberia (inset map). Fluctuations in the predicted distribution of *P. farinosa* during the Late Quaternary were incorporated in the phylogeographic model as exponential population decay at the onset of the Mid-Glacial (between 72 and 64 ka bp) and exponential growth during the Holocene (10 ka bp to present times), as indicated by the distribution through time analysis in a). Estimated growth rates are provided in Table 2. Symbols correspond to time (T), population sizes (N), migration rate (m), and exponential rates (r; see also Table 2).

demographic responses were lineage-specific were not supported, suggesting that the prior distributions for lineage-specific growth may be too narrow and restrictive. Taken together, these results indicate a significant Holocene expansion for *P. farinosa* as a whole. These results contrast with the expectation that the observed distribution of cold-adapted species currently fragmented in high altitude and latitude regions reflects the consequences of postglacial contraction processes (Hewitt 2004; Ehrich et al. 2007; Provan and Bennett 2008; Stewart et al. 2010). This classical scenario has indeed been supported in many case studies (e.g., Kropf et al. 2003; Dalén et al. 2007; Espíndola et al. 2012). For example, employing the same paleoclimatic data set used in our study (but at much lower resolution), Espíndola et al. (2012) identified significant postglacial contraction for *Trollius europaeus*, a cold-adapted plant species with distribution and climatic niche that largely overlap with those of *P. farinosa*. This discrepancy could be attributed to the fact that *T. europaeus* is a better competitor, found in comparatively more nutrient-rich habitats (Hitchmough 2003), attributes that may have allowed for its broader distribution during the last glacial period, followed by interglacial contraction. In stark

contrast, our study supports interglacial expansion for a cold-adapted species, providing the first empirical evidence for a model that had been proposed based mainly on theoretical considerations (Birks 2008; Stewart et al. 2010), as explained below.

The interglacial expansion hypothesis has been suggested as an alternative to the hypothesis of interglacial contraction for cold-adapted plants that may be either weak competitors and/or intolerant of drier climate (Schmitt 2007; Birks 2008). During the last glacial period, a large number of such cold-adapted species may have been excluded from the dry glacial steppes of central Europe (Harrison and Prentice 2003; Fletcher et al. 2010) that were mainly dominated by boreal dwarf shrubs (Tzedakis et al. 2013). Additionally, the cold-adapted plants that are predicted to have experienced postglacial expansion are currently not restricted to high alpine habitats, having wider ecological preferences than obligate alpine species (Ronikier et al. 2008b). Being tolerant of warm temperatures, these species may have initially persisted in lowland refugia during glacial maxima, from which they expanded when glaciers retreated and temperatures started to rise during the Holocene (Birks 2008), resulting in postglacial expansion (see Fig. 1, bottom panels). Nevertheless, while the leading edges of these species kept expanding to higher altitudes and latitudes during interglacials, competition from large herbs, shrubs, and trees tended to confine them to treeless refugia, such as river gravels, cliffs, and wetlands (Birks 2008). Indeed, *P. farinosa* is a weak competitor (Lindborg and Ehrlén 2002) that prefers mostly wet, open microhabitats (Theodoridis et al. 2013), factors that may not have allowed for an extensive European distribution during the last glaciation while favoring its postglacial expansion, as our results indicate (Fig. 7). Furthermore, *P. farinosa*'s tolerance for a range of temperatures (Theodoridis et al. 2013) may have enabled the persistence of populations at warmer, lower altitudes during interglacials, as currently observed in the Carpathians and Alps (Fig. 2), and the colonization of higher-latitude and altitude open habitats that became available following glacial retreat, resulting in its broad current range. Along with the expansion of *P. farinosa* into newly available habitats, the increasing temperature during the Holocene may have provided opportunities for temperate species to gradually invade the lowland habitats of *P. farinosa*, decreasing its lowland populations and restricting it to open habitats, such as calcareous fens (Hájek et al. 2011), where competitive temperate species do not typically occur (Hájek et al. 2006).

Multiple Sources of Postglacial Colonization

Given that European mountain systems were extensively glaciated during the LGM, it has been suggested that most plants specifically adapted to montane environments survived in peripheral and lowland refugia (Schönswetter et al. 2005; Holderegger and Thiel-Egenter 2009). Our results, namely, paleodistribution maps (Supplementary Fig. S1, available on Dryad) and strong lineage differentiation (Fig. 4a, Fig. 6), fit this scenario, suggesting that the southern lineages of *P. farinosa* probably survived the LGM in isolated regions of southern Europe in proximity of glaciated mountain systems (i.e., Carpathians, Alps, and Pyrenees), where wetter areas were available. These regions most likely served as multiple sources for postglacial colonization of the European mountains. Previous studies on mountain species have also suggested similar postglacial colonization patterns within the southern European mountain ranges (Després et al. 2002; Schmitt et al. 2006; Ronikier et al. 2008a; Schorr et al. 2013), however with no explicit analysis of population- and range-size dynamics, as performed in the present study.

The pre-LGM divergence of the Northern and Alpine lineages (Fig. 7b) and the predicted occurrence of *P. farinosa* in the British Isles during the LGM (Supplementary Fig. S1, available on Dryad) indicate that this latter region probably served as source for the colonization of Scandinavia and the Baltic region after the retreat of glaciers from the North Sea, a hypothesis that was previously suggested for other members of *Primula* sect. *Aleuritia* (Hultgård 1990). Corroborating this hypothesis, fossil seeds attributed to species of *Primula* sect. *Aleuritia* found in Pleistocene deposits of southern UK indicate that primroses occurred in this region during the last glacial period (Hultgård 1990). Additional palynological evidence for the occurrence of other cold-adapted species in the British Isles during the LGM (Kelly et al. 2010) indicates that this area might have served as a source for postglacial colonization of Northern Europe. Our findings thus lend further support to the hypothesis of northern cryptic glacial refugia for cold-adapted species (Tzedakis et al. 2013).

Potential Corridors That Enabled Migration among Refugia in Europe

Dispersal plays a key role in species and population persistence, especially in fragmented systems under rapid climatic change, via promoting (re)colonization of habitat patches and gene flow between isolated populations (Watkinson and Gill 2002). In our study, a part of France is predicted as climatically suitable for *P. farinosa* during the Mid-Glacial and LGM (Fig. 7 map inset; Supplementary Fig. S1, available on Dryad), although it currently harbors no known occurrences of the species. The predicted climatic suitability for *P. farinosa*, coupled with fossil evidence of a lowland steppe-tundra in this region during LGM (Peyron et al. 2005), suggests that suitable environmental corridors between the southwestern Alps and the Pyrenees may have existed during the LGM. These corridors may have allowed for dispersal across these regions through a patchy distribution of *P. farinosa* populations in Western Europe. The biogeographic link between the Alps and the Pyrenees is reflected in the inferred phylogeny of

Figure 5b, where the southwestern Alpine populations are more closely related to Iberian populations than to other Alpine populations. Previous studies have also provided genetic evidence for glacial links between the Pyrenees and the southwestern Alps (Després et al. 2002; Schmitt and Hewitt 2004; Schönswetter et al. 2009; Charrier et al. 2014) or even postglacial, long-distance dispersal between the two regions (Schönswetter et al. 2002). The results of our study further emphasize the importance of maintaining connectivity among isolated habitats for species persistence and diversity under climatic fluctuations, especially in fragmented systems such as the current habitats of cold-adapted species.

Implications for the Future of P. farinosa Under Global Change

Despite the suggested Holocene expansion of *P. farinosa* (Fig. 7) and the current predicted climatic suitability of several lowland regions in Europe for this cold-adapted species (Fig. 3), its conservation status in these regions raises serious concerns about negative human impacts on its persistence. In such climatically suitable, lowland regions, *P. farinosa* has gone extinct (e.g., Croatia: Topić and Stančić 2006) or almost extinct (e.g., Ukraine: Ziman et al. 2001; Didukh 2009; Hungary: Salamon-Albert and Morschhauser 2003; Poland: Gajewski et al. 2013; Denmark: Sørensen et al. 2014) in recent decades, mainly due to human-driven changes in its wetland microhabitats, such as fens. These changes might have allowed for the invasion of more competitive, temperate species, as discussed above. Furthermore, the species is listed as "vulnerable" in Great Britain (Cheffings et al. 2005), Slovakia (Turis et al. 2014), and Romania (Coldea et al. 2009). Thus, despite the recent expansion of *P. farinosa* supported by our analyses, its current threatened status in several countries indicates that modern human activities leading to the destruction of natural habitats may hinder the persistence of cold-adapted species and threaten their diversity.

Conclusions

In this article, we demonstrate the importance and utility of combining tools from different research fields, including ecology, population genomics, phylogenomics, and modeling, to test alternative hypotheses, estimate past demographic variables, and infer detailed phylogeographic scenarios of species evolution. Our results provide novel evidence to explain the persistence and range dynamics of cold-adapted species through Late-Quaternary climatic oscillations in Europe. In sharp contrast with the classic hypothesis of cold-adapted species attaining broader distributions during glacial maxima, this is the first study to provide sound evidence for the interglacial expansion of a cold-adapted plant at the European continental scale. By improving our understanding of past species responses to climatic oscillations, our results should allow us to make better predictions about how cold-adapted species might react to current and future human-driven changes.

Supplementary Material

Data available from the Dryad Digital Repository: http://dx.doi.org/10.5061/dryad.1fp80.

Funding

This work was supported by the Pro-Doc Research Module in Plant Sciences and Policy of the Swiss National Science Foundation [grant number 132471 to E.C. and C.R.], was affiliated with the Zurich-Basel Plant Science Center ProDoc Ph.D. Program in Plant Sciences & Policy, and was officially endorsed by DIVERSITAS-bioGENESIS; and by the Claraz Foundation and the Department of Systematic and Evolutionary Botany of the University of Zurich.

Acknowledgements

The authors would like to thank Per Toräng, Camille Madec, Mihai Puscas, Borja Jiménez Alfaro González, Nikolai Nikolov, Todor Karakiev, Liene Aunina, Michal Hajek, John Richards, Peter Schönswetter, and Gerald Schneeweiss for providing valuable information on species localities and help during field surveys; Christos Lataniotis for providing help with the development of scripts and the missing data index; the editors and referees for significantly improving the manuscript. The authors acknowledge the University of Zurich S3IT: Service and Support for Science IT, for providing the support and the computational resources that have contributed to the research results reported in this publication. URL: http://www.s3it.uzh.ch.

Appendix 1

Missing Data Distribution

Despite the increased power of resolution in population genetic, phylogeographic, and phylogenomic analyses afforded by high-throughput sequencing methods, data matrices generated using these recent technologies are plagued by the problem of missing data (Rubin et al. 2012; Eaton and Ree 2013; Huang and Knowles 2014). Such problem is particularly pronounced at higher levels of divergence among the populations under study, due to mutations in restriction or priming sites (i.e., recognition sequences) that may lead to nonrandom distribution of missing genotypes across the populations (Arnold et al. 2013). Structured patterns (nonrandom distribution) of

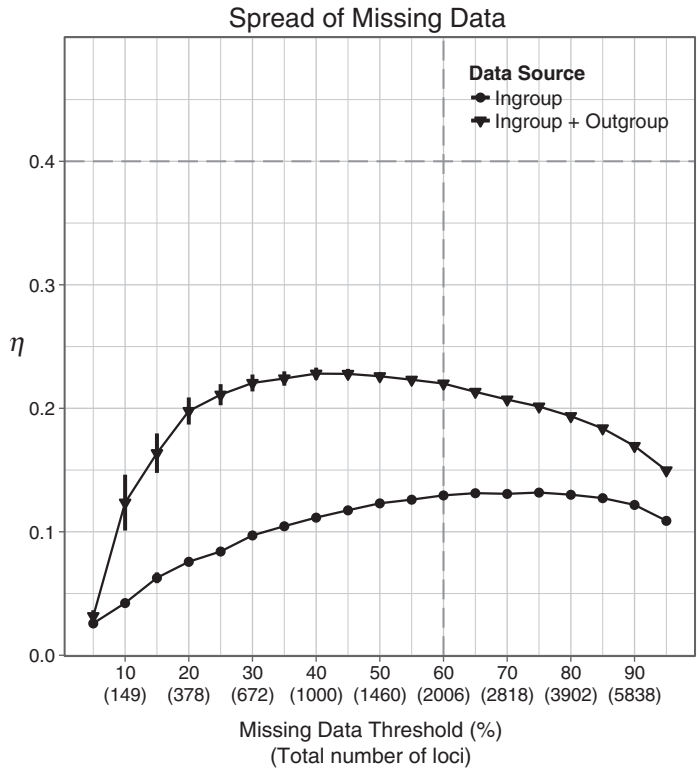

FIGURE A.1. Plot showing the values of η metric (i.e., Euclidean distance of observed missing data distribution from the expected nonstructured distribution across the data set) for different missing data thresholds. The missing data threshold corresponds to the percentage of genotypes a locus is allowed to lack. Lower values of the η metric indicate a nonstructured, random distribution of missing data across the four main lineages of P. farinosa, whereas higher values indicate a structured, nonrandom distribution. Each value of the η metric is an average value across all loci for the respective threshold. Vertical bars show standard error. The vertical dashed gray line represents the missing data threshold chosen for this study. Including loci under this threshold of missing data (60%) allowed us to recover a geographic genetic structure. The horizontal dashed grey line indicates a value of η where the distribution of missing genotypes in the dataset shows a strong bias. Values for η were obtained both for the ingroup (P. farinosa only) and the full (P. farinosa, P. exigua and P. frondosa) datasets. Numbers in parentheses show the total number of loci for each threshold.

missing data represent an important potential source of bias both in population structure (Clayton et al. 2005; Patterson et al. 2006) and phylogenomic (Rubin et al. 2012) inferences. On the other hand, a reduced data set consisting only of loci with low amounts of missing data results in lower accuracy of estimated phylogenetic and phylogeographic relationships by disproportionately excluding loci with the highest mutation rates (Huang and Knowles 2014). To date there is a lack of consensus on whether to include or exclude loci with large amounts of missing data in studies using RRL approaches.

The initial analysis of our genetic data set indicated a phylogeographic structure that was consistently recovered above a certain threshold of missing data defined as the allowed percentage of missing genotypes per locus. We thus explored our data set for potential structured patterns (i.e., nonrandom distribution) of missing data that could bias the phylogeographic signal. To facilitate the identification of such patterns, we developed a simple metric called η, analogous to Pearson's Chi-squared statistic, which quantifies the Euclidean distance of the observed data set from an expected data set with nonstructured (i.e., random) distribution of missing data across taxa. Consider a data set of one locus and two taxa where N_{t1} and N_{t2} are the total sample sizes per taxon and N_1 and N_2 the amount of missing genotypes for each population at a specific locus. Then, the observed ratios of missing data for each taxon are

$$P_1^{md} = \frac{N_1}{N_{t1}}, \quad P_2^{md} = \frac{N_2}{N_{t2}}$$

and the expected ratios given a nonstructured distribution (equal ratios across taxa) of missing data across the data set are given by

$$P_{1id}^{md} = \frac{\frac{N_{t1}}{N_{t1}+N_{t2}} \times (N_1+N_2)}{N_{t1}} = \frac{N_1+N_2}{N_{t1}+N_{t2}} = P_{2id}^{md}. \quad \text{(A.1)}$$

The normalized Euclidean distance of the observed from the expected data set equals

$$\eta = \sqrt{\frac{(P_1^{md} - P_{1id}^{md})^2}{n} + \frac{(P_2^{md} - P_{2id}^{md})^2}{n}}, \quad \text{(A.2)}$$

where n is the total number of taxa in the data set and $0 \leqslant \eta \leqslant 1$.

In order to apply the metric to our data set, we grouped taxa based on the respective geographic lineages. We thus defined four geographic groups for the ingroup (Alps, Carpathians, Iberia, and North) data set and a fifth one (the Balkans) for the outgroup data set. We calculated the η metric in Equation (A.2) for a range of missing data thresholds (from 0.5% to 95%, at 0.5% intervals) averaged across all loci at the respective threshold.

Missing Data Threshold Selection

Initial evaluation of different values of the η metric indicated that missing genotypes of loci with $\eta > 0.4$ showed a strongly biased distribution among the four groups. Additionally, our initial STRUCTURE and phylogenomic analyses revealed a geographic structure (K value and number of monophyletic clades) of the four *P. farinosa* lineages only after including loci above the threshold of 60% missing data per locus. The average η metric across all loci for the ingroup data set at the 60% missing data threshold was 0.129 (Fig. A.1), indicating a nonstructured distribution with relatively equal ratios of missing genotypes across the four groups. Similar η values were obtained between 50% and 90% of missing data thresholds. *Eta* values for the full data set were higher ($\eta = 0.22$ at 60% threshold; Fig. A.1), due to the fact that genotypes for many loci were missing mainly in the outgroup species. For the downstream analyses, we chose the 60% missing data threshold, representing the lowest threshold that allowed us to recover the above mentioned phylogeographic structure. The 60% threshold resulted in 37% of total missing data in the ingroup data set and 38.4% in the full data set. Additionally, the number of loci with $\eta > 0.4$ at 60% missing data threshold in the ingroup populations was very low (8 out of 2055).

References

Aguirre-Gutiérrez J., Carvalheiro L.G., Polce C., van Loon E.E., Raes N., Reemer M., Biesmeijer J.C. 2013. Fit-for-purpose: species distribution model performance depends on evaluation criteria—Dutch hoverflies as a case study. PLoS One 8:e63708.

Albert C.H., de Bello F., Boulangeat I., Pellet G., Lavorel S., Thuillet W. 2010. Sampling in ecology and evolution—bridging the gap between theory and practice. Ecography 33:1028–1037.

Allouche O., Tsoar A., Kadmon R. 2006. Assessing the accuracy of species distribution models: prevalence, kappa and the true skill statistic (TSS). J. Appl. Ecol. 43:1223–1232.

Alvarado-Serrano D.F., Knowles L.L. 2014. Ecological niche models in phylogeographic studies: applications, advances and precautions. Mol. Ecol. Resour. 14:233–248.

Araújo M.B., New M. 2007. Ensemble forecasting of species distributions. Trends Ecol. Evol. 22:42–47.

Arnold B., Corbett-Detig R.B., Hartl D., Bomblies K. 2013. RADseq underestimates diversity and introduces genealogical biases due to nonrandom haplotype sampling. Mol. Ecol. 22:3179–3190.

Avise J.C. 2009. Phylogeography: retrospect and prospect. J. Biogeogr. 36:3–15.

Barbet-Massin M., Jiguet F., Albert C.H., Thuiller W. 2012. Selecting pseudo-absences for species distribution models: how, where and how many? Methods Ecol. Evol. 3:1–12.

Beaumont M.A., Zhang W.Y., Balding D.J. 2002. Approximate Bayesian computation in population genetics. Genetics 162: 2025–2035.

Beaumont M.A. 2008. Joint determination of topology, divergence time, and immigration in population trees. In: Matsumura S., Forster P., Renfrew C., editors. Simulations, genetics and human prehistory. Cambridge (UK): McDonald Institute Monographs. p. 135–154.

Beaumont M.A. 2010. Approximate Bayesian computation in evolution and ecology. Annu. Rev. Ecol. Evol. Syst. 41:379–406.

Birks H.H. 2008. The Late-Quaternary history of arctic and alpine plants. Plant Ecol. Divers. 2:135–146.

Bouckaert R.R. 2010. DensiTree: making sense of sets of phylogenetic trees. Bioinformatics 26:1372–1373.

Breiman L. 2001. Random forests. Mach. Learn. 45:5–32.

Browning S., Weir B. 2010. Population structure with localized haplotype clusters. Genetics 185:1337–1344.

Bruun H.G. 1932. Cytological studies in *Primula*. Symb. Bot. Ups. 1: 56–67.

Bryant D., Bouckaert R., Felsenstein J., Rosenberg N.A., RoyChoudhury A. 2012. Inferring species trees directly from biallelic genetic markers: bypassing gene trees in a full coalescent analysis. Mol. Biol. Evol. 29:1917–1932.

Brys R., Jacquemyn H. 2009. Biological flora of the British Isles: *Primula veris* L. J. Ecol. 97:581–600.

Carstens B., Lemmon A.R., Lemmon E.M. 2012. The promises and pitfalls of next-generation sequencing data in phylogeography. Syst. Biol. 61:713–715.

Catchen J., Hohenlohe P.A., Bassham S., Amores A., Cresko W.A. 2013. Stacks: an analysis tool set for population genomics. Mol. Ecol. 22:3124–3140.

Charrier O., Dupont P., Pornon A., Escaravage N. 2014. Microsatellite marker analysis reveals the complex phylogeographic history of *Rhododendron ferrugineum* (Ericaceae) in the Pyrenees. PLoS One 9:e92976.

Cheffings C.M., Farrell L., Dines T.D., Jones R.A., Leach S.J., McKean D.R., Pearman D.A., Preston C.D., Rumsey F.J., Taylor I. 2005. The vascular plant red data list for Great Britain. Species status. Joint Nat. Conserv. Committee 7:1–116.

Clayton D.G., Walker N.M., Smyth D.J., Pask R., Cooper J.D., Maier L.M., Smink L.J., Lam A.C., Ovington N.R., Stevens H.E., Nutland S., Howson J.M.M., Faham M., Moorhead M., Jones H.B., Falkowski M., Hardenbol P., Willis T.D., Todd J.A. 2005. Population structure, differential bias and genomic control in a large-scale, case–control association study. Nat. Genet. 37:1243–1246.

Coldea G., Stoica I.A., Puşcaş M., Ursu T., Oprea A., The IntraBioDiv Consortium. 2009. Alpine-subalpine species richness of the Romanian Carpathians and the current conservation status of rare species. Biodivers. Conserv. 18:1441–1458.

Conrad D.F., Jakobsson M., Coop G., Wen X., Wall J.D., Rosenberg N.A., Pritchard J.K. 2006. A worldwide survey of haplotype variation and linkage disequilibrium in the human genome. Nat. Genet. 38: 1251–1260.

Cornuet J.M., Pudlo P., Veyssier J., Dehne-Garcia A., Gautier M., Leblois R., Marin J.M., Estoup A. 2014. DIYABC v2.0: a software to make approximate Bayesian computation inferences about population history using Single Nucleotide Polymorphism, DNA sequence and microsatellite data. Bioinformatics 30:1187–1189.

Crandall E.D., Sbrocco E.J., DeBoer T.S., Barber P.H., Carpenter K.E. 2012. Expansion dating: calibrating molecular clocks in marine species from expansions onto the Sunda Shelf following the Last Glacial Maximum. Mol. Biol. Evol. 29:707–719.

Crawford R.M.M. 2008. Cold climate plants in a warmer world. Plant Ecol. Divers. 1:285–297.

Csilléry K., Blum M.G., Gaggiotti O.E., François O. 2010. Approximate Bayesian computation (ABC) in practice. Trends Ecol. Evol. 25: 410–418.

Csilléry K., François O., Blum M.G.B. 2012. abc: an R package for Approximate Bayesian computation (ABC). Methods Ecol. Evol. 3:475–479.

Dalén L., Nyström V., Valdiosera C., Germonpré M., Sablin M., Turner E., Angerbjörn A., Arsuaga J.L., Götherström A. 2007. Genetic contribution of Arctic population in the South: post recolonisation of the Arctic fox in Europe. Proc. Natl. Acad. Sci. USA. 104:6726–6729.

Darwin C. 1859. On the origin of species by means of natural selection, or the preservation of favoured races in the struggle for life. London (UK): John Murray. p. 364–382.

Davey J.W., Hohenlohe P.A., Etter P.D., Boone J.Q., Catchen J.M., Blaxter M.L. 2011. Genome-wide genetic marker discovery and genotyping using next-generation sequencing. Nat. Rev. Genet. 12:499–510.

Dawson T.P., Jackson S.T., House J.I., Prentice I.C., Mace G.M. 2011. Beyond predictions: biodiversity conservation in a changing climate. Science 332:53–58.

de Vos J.M., Hughes C.H., Schneeweiss G.M., Moore B.R., Conti E. 2014. Heterostyly accelerates diversification via reduced extinction in primroses. Proc. R. Soc. B 281:20140075.

Després L., Loriot S., Gaudeul M. 2002. Geographic pattern of genetic variation in the European globeflower *Trollius europaeus* L. (Ranunculaceae) inferred from amplified fragment length polymorphism markers. Mol. Ecol. 11:2337–2347.

Didukh YaP. 2009. Red data book of Ukraine. Vegetable Kingdom. Kyiv (UA): Globalconsulting.

Dullinger S., Gattringer A., Thuiller W., Moser D., Zimmermann N.E., Guisan A., Willner W., Plutzar C., Leitner M., Mang T., Caccianiga M., Dirnböck T., Ertl S., Fischer A., Lenoir J., Svenning J.C., Psomas A., Schmatz D.R., Silc U., Vittoz P., Hülber K. 2012. Extinction debt of high-mountain plants under twenty-first-century climate change. Nat. Clim. Change 2:619–622.

Doyle J.J., Doyle J.L. 1990. Isolation of plant DNA from fresh tissues. Focus 12:13–15.

Eaton D.A.R., Ree R.H. 2013. Inferring phylogeny and introgression using RADseq data: an example from flowering plants (*Pedicularis*: Orobanchaceae). Syst. Biol. 62:689–706.

Edwards S.V., Liu L., Pearl D.K. 2007. High-resolution species trees without concatenation. Proc. Natl. Acad. Sci. USA. 104:5936–5941.

Ehlers J., Gibbard P.L., Hughes P.D. 2011. Quartenary glaciations—extent and chronology. Vol. 15, 1st ed. Elsevier. Available from URL: http://booksite.elsevier.com/9780444534477/digital_maps.php.

Ehrich D., Gaudeul M., Assefa A., Koch M.A., Mummenhoff K., Nemomissa S., Intrabiodiv Consortium, Brochmann C. 2007. Genetic consequences of Pleistocene range shifts: contrast between the Arctic, the Alps and the East African mountains. Mol. Ecol. 16:2542–2559.

Elith J., Graham C., The NCEAS Species Distribution Modelling Group. 2006. Novel methods improve prediction of species' distributions from occurrence data. Ecography 29:129–151.

Emerson K.J., Merz C.R., Catchen J.M., Hohenlohe P.A., Cresko W.A., Bradshaw W.E., Holzapfel C.M. 2010. Resolving postglacial phylogeography using high-throughput sequencing. Proc. Natl. Acad. Sci. USA. 107:16196–16200.

Engler R., Randin C.F., Thuiller W., Dullinger S., Zimmermann N.E., Araújo M.B., Pearman P.B., Le Lay G., Piedallu C., Albert C.H., Choler P., Coldea G., De Lamo X., Dirnböck T., Gégout J.C., Gómez-García D., Grytnes J.A., Heegaard E., Høistad F., Nogués-Bravo D., Normand S., Puşcaş M., Sebastiàn M.T., Stanisci A., Theurillat J.P., Trivedi M.R., Vittoz P., Guisan A. 2011. 21st century climate change threatens mountain flora unequally across Europe. Glob. Chang. Biol. 17:2330–2341.

Espíndola A., Pellissier L., Maiorano L., Hordijk W., Guisan A., Alvarez N. 2012. Predicting present and future intra-specific genetic structure through niche hindcasting across 24 millennia. Ecol. Lett. 15:649–657.

Estoup A., Beaumont M., Sennedot F., Moritz C., Cornuet J.M. 2004. Genetic analysis of complex demographic scenarios: spatially expanding populations of the cane toad, *Bufo marinus*. Evolution 58:2021–2036.

Etterson J.R. 2008 Evolution in response to climate change. In: Carroll S.P., Fox C.W., editors. Conservation biology evolution in action. Kentucky (USA): Oxford University Press. p. 145–163.

Evanno G., Regnaut S., Goudet J. 2005. Detecting the number of clusters of individuals using the software STRUCTURE: a simulation study. Mol. Ecol. 14:2611–2620.

Excoffier L., Dupanloup I., Huerta-Sánchez E., Sousa V.C., Foll M. 2013. Robust demographic inference from genomic and SNP data. PLoS Genet. 9:e1003905.

Fielding A.H., Bell J.F. 1997. A review of methods for the assessment of prediction errors in conservation presence/absence models. Environ. Conserv. 24:38–49.

Fletcher W., Sánchez Goñi M.F., Allen J.M.R., Cheddadi R., Combourieu-Nebout N., Huntley B., Lawson I., Londeix L., Magri D., Margari V., Müller U.C., Naughton F., Novenko E., Roucoux K., Tzedakis P.C. 2010. Millennial-scale variability during the last glacial in vegetation records from Europe. Quat. Sci. Rev. 29;2839–2864.

François O., Blum M.G.B., Jakobsson M., Rosenberg N.A. 2008. Demographic history of European populations of *Arabidopsis thaliana*. PLoS Genet. 4:e1000075.

Friedman J.H. 2001. Greedy function approximation: a gradient boosting machine. Ann. Stat. 29:1189–1232.

Gajewski Z., Sitek E., Stolarczyk P., Nowak B., Kapała K. 2013. A current status of the population of *Primula farinosa* L. (Primulaceae) at the only one known site in Poland. Pol. J. Ecol. 61:797–804.

Gavin D.G., Fitzpatrick M.C., Gugger P.F., Heath K.D., Rodríguez-Sánchez F., Dobrowski S.Z., Hampe A., Hu F.S., Ashcroft M.B., Bartlein P.J., Blois J.L., Carstens B.C., Davis E.B., de Lafontaine G., Edwards M.E., Fernandez M., Henne P.D., Herring E.M., Holden Z.A., Kong W.S., Liu J., Magri D., Matzke N.J., McGlone M.S., Saltré F., Stigall A.L., Tsai Y.H.E., Williams J.W. 2014. Climate refugia: joint inference from fossil records, species distribution models and phylogeography. New Phytol. 204:37–54.

Gossmann T.I., Song B.H., Windsor A.J., Mitchell-Olds T., Dixon C.J., Kapralov M.V., Filatov D.A., Eyre-Walker A. 2010. Genome wide analyses reveal little evidence for adaptive evolution in many plant species. Mol. Biol. Evol. 27:1822–1832.

Guggisberg A., Mansion G., Kelso S., Conti E. 2006. Evolution of biogeographic patterns, ploidy levels, and breeding systems in a diploid–polyploid species complex of *Primula*. New Phytol. 171: 617–632.

Guggisberg A., Mansion G., Conti E. 2009. Disentangling reticulate evolution in an arctic–alpine polyploid complex. Syst. Biol. 58: 55–73.

Guisan A., Thuiller W. 2005. Predicting species distribution: offering more than simple habitat models. Ecol. Lett. 8:993–1009.

Haasl R.J., Payseur B.A. 2011. Multi-locus inference of population structure: a comparison between single nucleotide polymorphisms and microsatellites. Heredity 106:158–171.

Hájek M., Horsák M., Hájková P., Dítě D. 2006. Habitat diversity of central European fens in relation to environmental gradients and an effort to standardise fen terminology in ecological studies. Perspect. Plant Ecol. Evol. Syst. 8:97–114.

Hájek M., Horsák M., Tichý L., Hájková P., Dítě D., Jamrichová E. 2011. Testing a relict distributional pattern of fen plant and terrestrial snail species at the Holocene scale: a null model approach. J. Biogeogr. 38:742–755.

Hambler D.J., Dixon J.M. 2003. *Primula farinosa* L. J. Ecol. 91:694–705.

Harrison S.P., Prentice I.C. 2003. Climate and CO_2 controls on global vegetation distribution at the last glacial maximum: analysis based on palaeovegetation data, biome modelling and palaeoclimate simulations. Glob. Chang. Biol. 9:983–1004.

Hastie T., Tibshirani R. 1990. Generalized additive models. Stat. Sci. 1:297–318.

Hewitt G.M. 1996. Some genetic consequences of ice ages, and their role in divergence and speciation. Biol. J. Lin. Soc. 58:247–276.

Hewitt G.M. 1999. Post-glacial re-colonization of European biota. Biol. J. Linn. Soc. 68:87–112.

Hewitt G.M. 2000. The genetic legacy of the Quaternary ice ages. Nature 405:907–913.

Hewitt G.M. 2004. Genetic consequences of climatic oscillations in the Quaternary. Philos. Trans. R. Soc. B 359:183–195.

Hickerson M.J., Carstens B.C., Cabender-Bares J., Crandall K.A., Graham C.H., Johnson J.B., Rissler L., Victoriano P.F., Yoder A.D. 2010. Phylogeography's past, present, and future: 10 years after Avise, 2000. Mol. Phylogenet. Evol. 54:291–301.

Hijmans R.J., Cameron S.E., Parra J.L., Jones P.G., Jarvis A. 2005. Very high resolution interpolated climate surfaces for global land areas. Int. J. Climatol. 25:1965–1978.

Hitchmough J.D. 2003. Effects of sward height, gap size, and slug grazing on emergence and establishment of *Trollius europaeus* (Globeflower). Restor. Ecol. 11:20–28.
Hoareau T.B. 2015. Late-glacial demographic expansion motivates a clock overhaul for population genetics. Syst. Biol. 65:449–464.
Holderegger R., Thiel-Egenter C. 2009. A discussion of different types of glacial refugia used in mountain biogeography and phylogeography. J. Biogeogr. 36:476–480.
Howard C., Stephens P.A., Pearce-Higgins J.W., Gregory R.D., Willis S.G. 2014. Improving species distribution models: the value of data on abundance. Methods Ecol. Evol. 5:506–513.
Hultgård U.M. 1990. Polyploidy and differentiation in northern European populations of *Primula* subgenus *Aleuritia*. Sommerfeltia 11:117–135.
Huang H., Knowles L. 2014. Unforeseen consequences of excluding missing data from next-generation sequences: simulation study of RAD sequences. Syst. Biol. 65:357–365.
Jakobsson M., Rosenberg N.A. 2007. CLUMPP: a cluster matching and permutation program for dealing with label switching and multimodality in analysis of population structure. Bioinformatics 23:1801–1806.
Kalinowski S.T. 2004. Counting alleles with rarefaction: private alleles and hierarchical sampling designs. Conserv. Genet. 5:539–543.
Kelly A., Charman D., Newnham R.M. 2010. A Last Glacial Maximum pollen record from Bodmin Moor showing a possible cryptic northern refugium in southwest England. J. Quat. Sci. 25:296–308.
Knowles L.L. 2009. Statistical phylogeography. Annu. Rev. Ecol. Syst. 40:593–612.
Körner C. 2003. Alpine plant life—functional plant ecology of high mountain ecosystems. Heidelberg: Springer.
Kropf M., Kadereit J.W., Comes H.P. 2003. Differential cycles of range contraction and expansion in European high mountain plants during the Late Quaternary: insights from *Pritzelago alpina* (L.) O. Kuntze (Brassicaceae). Mol. Ecol. 12:931–949.
Lachance J., Tishkoff S.A. 2013. SNP ascertainment bias in population genetic analyses: why it is important and how to correct it. BioEssays 35:780–786.
Landis J.R., Koch G.G. 1977. The measurement of observer agreement for categorical data. Biometrics 33:159–174.
Lavergne S., Mouquet N., Thuiller W., Ronce O. 2010. Biodiversity and climate change: integrating evolutionary and ecological responses of species and communities. Ann. Rev. Ecol. Evol. Syst. 41: 321–350.
Leaché A.D., Fujita M.K., Minin V., Bouckaert R. 2014. Species delimitation using genome-wide SNP data. Syst. Biol. 63:534–542.
Lemmon A.R., Lemmon E.M. 2012. High-throughput identification of informative nuclear loci for shallow-scale phylogenetics and phylogeography. Syst. Biol. 61:745–761.
Lemmon E.M., Lemmon A.R. 2013. High-throughput genomic data in systematics and phylogenetics. Annu. Rev. Ecol. Evol. Syst. 44: 727–744.
Leuenberger C., Wegmann D. 2010. Bayesian computation and model selection without likelihoods. Genetics 184:243–252.
Lindborg R., Ehrlén J. 2002. Evaluating the extinction risk of a perennial herb: demographic data versus historical records. Conserv. Biol. 16:683–690.
Lischer H.E.L., Excoffier L., Heckel G. 2014. Ignoring heterozygous sites biases phylogenomic estimates of divergence times: implications for the evolutionary history of *Microtus* voles. Mol. Biol. Evol. 31: 817–831.
Liu C., Berry P.M., Dawson T.P., Pearson R.G. 2005. Selecting thresholds of occurrence in the prediction of species distributions. Ecography 28:385–393.
Maiorano L., Cheddadi R., Zimmermann N.E., Pellissier L., Petitpierre B., Pottier J., Laborde H., Hurdu B.I., Pearman P.B., Psomas A., Singarayer J.S., Broennimann O., Vittoz P., Dubuis A., Edwards M.E., Binney H.A., Guisan A. 2013. Building the niche through time: using 13,000 years of data to predict the effects of climate change on three tree species in Europe. Glob. Ecol. Biogeogr. 22: 302–317.
McTavish E.J., Hillis D.M. 2015. How do SNP ascertainment schemes and population demographics affect inferences about population history? BMC Genomics 16:266.
McCullagh P., Nelder J.A. 1989. Generalized linear models. 2nd edn. London (UK): Chapman & Hall.
Miller N., Estoup A., Toepfer S., Bourguet D., Lapchin L., Derridj S., Kim K.S., Reynaud P., Furlan L., Guillemaud T. 2005. Multiple transatlantic introductions of the western corn rootworm. Science 310:992.
Minoche A.E., Dohm J.C., Himmelbauer H. 2011. Evaluation of genomic high-throughput sequencing data generated on Illumina HiSeq and Genome Analyzer systems. Genome Biol. 12:R112.
Muster C., Berendonk T.U. 2006. Divergence and diversity: lessons from an arctic–alpine distribution (*Pardosa saltuaria* group, Lycosidae). Mol. Ecol. 15:2921–2933.
Nogués-Bravo D. 2009. Predicting the past distribution of species climatic niches. Glob. Ecol. Biogeogr. 18:521–531.
Pakeman R.J. 2001. Plant migration rates and seed dispersal mechanisms. J. Biogeogr. 28:795–800.
Patiño J., Carine M., Mardulyn P., Devos N., Mateo R.G., González-Mancebo J.M., Shaw A.J., Vanderpoorten A. 2015. Approximate Bayesian computation reveals the crucial role of oceanic islands for the assembly of continental biodiversity. Syst. Biol. 64:579–589.
Patterson N., Price A.L., Reich D. 2006. Population structure and eigenanalysis. PLoS Genet. 22:e190.
Patsiou T.S., Conti E., Zimmermann N.E., Theodoridis S., Randin C.F. 2014. Topo-climatic microrefugia explain the persistence of a rare endemic plant in the Alps during the last 21 millennia. Glob. Chang. Biol. 20:2286–2300.
Pearce J., Ferrier S. 2000. Evaluating the predictive performance of habitat models developed using logistic regression. Ecol. Model. 133:225–245.
Peyron O., Bégeot C., Brewer S., Heiri O., Magny M., Millet L., Ruffaldi P., van Campo E., Yu G. 2005. Lateglacial climate in the Jura mountains (France) based on different quantitative reconstruction approaches from pollen, lake-levels, and chironomids. Quat. Res. 64:197–211.
Phillips S.J., Anderson R.P., Schapire R.E. 2006. Maximum entropy modeling of species geographic distributions. Ecol. Model. 190: 231–259.
Pickrell J.K., Pritchard J.K. 2012. Inference of population splits and mixtures from genome-wide allele frequency data. PLoS Genet. 8:e1002967.
Pritchard J.K., Seielstad M.T., Perez-Lezaun A., Feldman M.W. 1999. Population growth of human Y chromosomes: a study of Y chromosome microsatellites. Mol. Biol. Evol. 16:1791–1798.
Pritchard J.K., Stephens M., Donnelly P. 2000. Inference of population structure using multilocus genotype data. Genetics 155:945–959.
Provan J., Bennett K.D. 2008. Phylogeographic insights into cryptic glacial refugia. Trends Ecol. Evol. 23:564–571.
Rambaut A., Drummond A. 2008. TreeAnnotator (Version 1.8). Available from URL: http://beast.bio.ed.ac.uk/TreeAnnotator.
Rambaut A., Suchard M.A., Xie D., Drummond A.J. 2014. Tracer (Version 1.6). Available from URL: http://beast.bio.ed.ac.uk/Tracer.
Randin C.F., Dirnböck T., Dullinger S., Zimmermann N.E., Zappa M., Guisan A. 2006. Are niche-based species distribution models transferable in space? J. Biogeogr. 33:1689–1703.
Ray N., Wegmann D., Fagundes N.J., Wang S., Ruiz-Linares A., Excoffier L. 2010. A statistical evaluation of models for the initial settlement of the American continent emphasizes the importance of gene flow with Asia. Mol. Biol. Evol. 27:337–345.
R Development Core Team. 2013. R: a language and environment for statistical computing. Vienna, Austria: The R Foundation for Statistical Computing.
Rheindt F.E., Fujita M.K., Wilton P.R., Edwards S.V. 2014. Introgression and phenotypic assimilation in *Zimmerius* flycatchers (Tyrannidae): population genetic and phylogenetic inferences from genome-wide SNPs. Syst. Biol. 63:134–152.
Richards C.L., Carstens B.C., Knowles L.L. 2007. Distribution modelling and statistical phylogeography: an integrative framework for generating and testing alternative biogeographical hypotheses. J. Biogeogr. 34:1833–1845.
Richards J. 2003. Primula. London (UK): BT Batsford Ltd.
Ronikier M., Cieslak E.M., Korbecka G. 2008a. High genetic differentiation in the alpine plant *Campanula alpina* Jacq.

(Campanulaceae): evidence for glacial survival in several Carpathian regions and long-term isolation between the Carpathians and the Alps. Mol. Ecol. 17:1763–1775.

Ronikier M., Costa A., Fuertes Aguilar J., Nieto Feliner G., Küpfer F., Mirek Z. 2008b. Phylogeography of *Pulsatilla vernalis* (L.) Mill. (Ranunculaceae): chloroplast DNA reveals two evolutionary lineages across central Europe and Scandinavia. J. Biogeogr. 35:1650–1664.

Rubin B.E., Ree R.H., Moreau C.S. 2012. Inferring phylogenies from RAD sequence data. PLoS One 7:e33394.

Salamon-Albert É., Morschhauser T. 2003. Habitat preferences of a unique specialist plant species (*Primula farinosa* subsp. *alpigena*) in Hungary. Acta Bot. Hung. 45:193–215.

Schmatz D.R., Luterbacher J., Zimmermann N.E., Pearman P.B. In revision. Gridded climate data from 5 GCMs of the Last Glacial Maximum downscaled to 30 arc seconds for Europe. Clim. Past.

Schmitt T., Hewitt G.M. 2004. Molecular biogeography of the arctic–alpine disjunct burnet moth species *Zygaena exulans* (Zygaenidae, Lepidoptera) in the Pyrenees and Alps. J. Biogeogr. 31:885–893.

Schmitt T., Hewitt G.M., Müller P. 2006. Disjunct distributions during glacial and interglacial periods in mountain butterflies: *Erebia epiphron* as an example. J. Evol. Biol. 19:108–113.

Schmitt T. 2007. Molecular biogeography of Europe: pleistocene cycles and postglacial trends. Front. Zool. 4:11.

Schönswetter P., Tribsch A., Barfuss M., Nikfeld H. 2002. Several Pleistocene refugia detected in the high aline plant *Phyteuma globulariifolium* Sternb. & Hoppe (Campanulaceae) in the European Alps. Mol. Ecol. 11:2637–2647.

Schönswetter P., Stehlik I., Holderegger R., Tribsch A. 2005. Molecular evidence for glacial refugia of mountain plants in the European Alps. Mol. Ecol. 14:3547–3555.

Schönswetter P., Solstad H., Escobar García P., Elven R. 2009. A combined molecular and morphological approach to the taxonomically intricate European mountain plant *Papaver alpinum* s.l. (Papaveraceae). Taxa or informal phylogeographical groups? Taxon 58:1326–1343.

Schorr G., Pearman P.B., Guisan A., Kadereit J.W. 2013. Combining palaeodistribution modelling and phylogeographical approaches for identifying glacial refugia in Alpine *Primula*. J. Biogeogr. 40: 1947–1960.

Shapiro B., Drummond A.J., Rambaut A., Wilson M.C., Matheus P.E., Sher A.V., Pybus O.G., Gilbert M.T.P., Barnes I., Binladen J., Willerslev E., Hansen A.J., Baryshnikov G.F., Burns J.A., Davydov S., Driver J.C., Froese D.G., Harington C.R., Keddie G., Kosintsev P., Kunz M.L., Martin L.D., Stephenson R.O., Storer J., Tedford R., Zimov S., Cooper A. 2004. Rise and fall of the Beringian steppe bison. Science 306:1561–1565.

Singarayer J.S., Valdes P.J. 2010. High-latitude climate sensitivity to ice-sheet forcing over the last 120 kyr. Quat. Sci. Rev. 29:43–55.

Sørensen S.B., Larsen B., Orabi J., Ørgaard M. 2014. *Primula farinosa* in Denmark; genetic diversity and population management. Nordic J. Bot. 8:1–8.

Stamatakis A., Hoover P., Rougement J. 2008. A rapid bootstrap algorithm for the RAxML web-servers. Syst. Biol. 57:758–771.

Stamatakis A. 2014. RAxML version 8: a tool for phylogenetic analysis and post-analysis of large phylogenies. Bioinformatics 30:1312–1313.

Stewart J.R., Lister A.M., Barnes I., Dalén L. 2010. Refugia revisited: individualistic responses of species in space and time. Proc. R. Soc. B 277:661–671.

Sukumaran J., Holder M.T. 2010. DendroPy: a Python library for phylogenetic computing. Bioinformatics 26:1569–1571.

Svenning J.C., Fløjgaard C., Marske K.A., Nógues-Bravo D., Normand S. 2011. Applications of species distribution modeling to paleobiology. Quat. Sci. Rev. 30:2930–2947.

Taberlet P., Cheddadi R. 2003. Quaternary refugia and persistence of biodiversity. Science 297:2009–2010.

Theodoridis S., Randin C., Broennimann O., Patsiou T., Conti E. 2013. Divergent and narrower climatic niches characterize polyploid species of European primroses in *Primula* sect. *Aleuritia*. J. Biogeogr. 40:1278–1289.

Topić J., Stančić Z. 2006. Extinction of fen and bog plants and their habitats in Croatia. Biodivers. Conserv. 15:3371–3381.

Turis P., Kliment J., Feráková V., Dítě D., Eliáš jun P., Hrivnák R., Košťál J., Šuvada R., Mráz P., Bernátová D. 2014. Red list of vascular plants of the Carpathian part of Slovakia. Thaiszia J. Bot. 24:35–87.

Tzedakis P., Emerson B., Hewitt G. 2013. Cryptic or mystic? Glacial tree refugia in northern Europe. Trends Ecol. Evol. 28:696–704.

Urbanska K.M., Schutz M. 1986. Reproduction by seed in alpine plants and revegetation research above timberline. Bot. Helv. 96: 43–60.

Watkinson A.R., Gill J.A. 2002. Climate change and dispersal. In: Bullock J.M., Kenward R.E., Hails R.S., editors. Dispersal ecology. Oxford (UK): Blackwell Science Publishing. p. 45–56.

Wegmann D., Excoffier L. 2010. Bayesian inference of the demographic history of chimpanzees. Mol. Biol. Evol. 27:1425–1435.

Wegmann D., Leuenberger C., Neuenschwander S., Excoffier L. 2010. ABCtoolbox: a versatile toolkit for approximate Bayesian computations. BMC Bioinformatics 11:1–7.

Westergaard K.B., Alsos I.G., Popp M., Engelskjøn T., Flatberg K.I., Brochmann C. 2010. Glacial survival may matter after all: nunatak signatures in the rare European populations of two west-arctic species. Mol. Ecol. 20:376–393.

Wiens J.J. 2011. The niche, biogeography and species interactions. Philos. Trans. R. Soc. B 366:2336–2350.

Willis K.J., Whittaker R.J. 2000. The refugial debate. Science 287: 1406–1407.

Zhang L.B., Comes H.P., Kadereit J.W. 2001. Phylogeny and quarternary history of the European montane/alpine endemic *Soldanella* (Primulaceae) based on ITS and AFLP variation. Am. J. Bot. 88: 2331–2345.

Ziman S., Coldea G., Cristea V., Boscaiu N., Novosad V. 2001. *Primula farinosa* L. and the relict community *Caricetum davallianae* in the Carpathians and their protection. Bull. Natl. Sci. Natl. Mus. 1: 196–199.